Available online at www.sciencedirect.com
SCIENCE DIRECT®
ELSEVIER
Earth-Science Reviews 64 (2004) 157–187
EARTH-SCIENCE REVIEWS
www.elsevier.com/locate/earscirev

A revised morpho- and chronostratigraphy of the Late and Middle Pleistocene coral reef terraces on Southern Barbados (West Indies)

G. Schellmann[a,*], U. Radtke[b]

[a] Department of Geography, University of Bamberg, Am Kranen 1, D-96045 Bamberg, Germany
[b] Department of Geography, University of Cologne, D-50923 Köln, Germany

Received 10 December 2002; accepted 10 April 2003

Abstract

The Barbados coral reef terraces are one of the few type localities worldwide that provide insights into interglacial sea level change during the Late and Middle Pleistocene. Several sea level estimates have been established since the late 1960s and each has contributed to the "Barbados Model" of sea level change. This paper presents new morpho- and chonostratigraphic data from the Barbados coral reef terraces developed over the last 12 years. The work is based on significant advances in Electron Spin Resonance (ESR)-dating of fossil coral, air photo interpretation, and a greatly improved geomorphic map of preserved fossil beach formations and reef terraces above present sea level. The need for a revision of past published morpho- and chronostratigraphies is best demonstrated on the southern part of the island. The morpho- and chronostratigraphic sequence in this region is both more complex and diverse than has been assumed so far. The revised morphostratigraphy presented here includes a differentiation of coral reef terraces, wave-cut platforms and other erosive features, such as notches and cliffs. Our study of these geomorphic features, combined with new numeric dating results (ESR, U/Th), enable a revised estimate of the spatial and temporal variation in tectonic uplift rate within south Barbados. These new rates are an essential requirement for more precise glacio-eustatic sea level reconstructions during the Late and Middle Pleistocene from this region.

Keywords: Barbados; Coral reef terraces; ESR ages; Wave-cut platforms; Notches; Palaeo sea level

1. Introduction

Barbados is located in the eastern Caribbean, approx. 160 km east of the Lesser Antilles volcanic arc (Fig. 1), and extends from 13°02′ to 13°10′ N to 59°25′ to 59°39′ W. The island has a north–south extent of 32 km and an east–west extent of 24 km, an area of approx. 430 km^2, and approx. 95 km of coastline. Geographically, Barbados belongs to the Lesser Antilles, the "islands above the wind", located within the belt of northeastern trade winds. Therefore, the eastern Atlantic shore of Barbados experiences higher-energy wave action compared to the more protected leeward Caribbean coastline.

The island is geologically and tectonically distinct from the other volcanic and coral limestone islands of the Lesser Antilles. Most importantly, it is located in a region where large amounts of oceanic sediment have been scraped off the ocean floor to form an accretionary prism approx. 20 km in thickness. This sedi-

* Corresponding author. Fax: +49-951-8631193.
E-mail addresses: gerhard.schellmann@ggeo.uni-bamberg.de (G. Schellmann), u.radtke@uni-koeln.de (U. Radtke).

0012-8252/$ - see front matter © 2003 Elsevier B.V. All rights reserved.
doi:10.1016/S0012-8252(03)00043-6

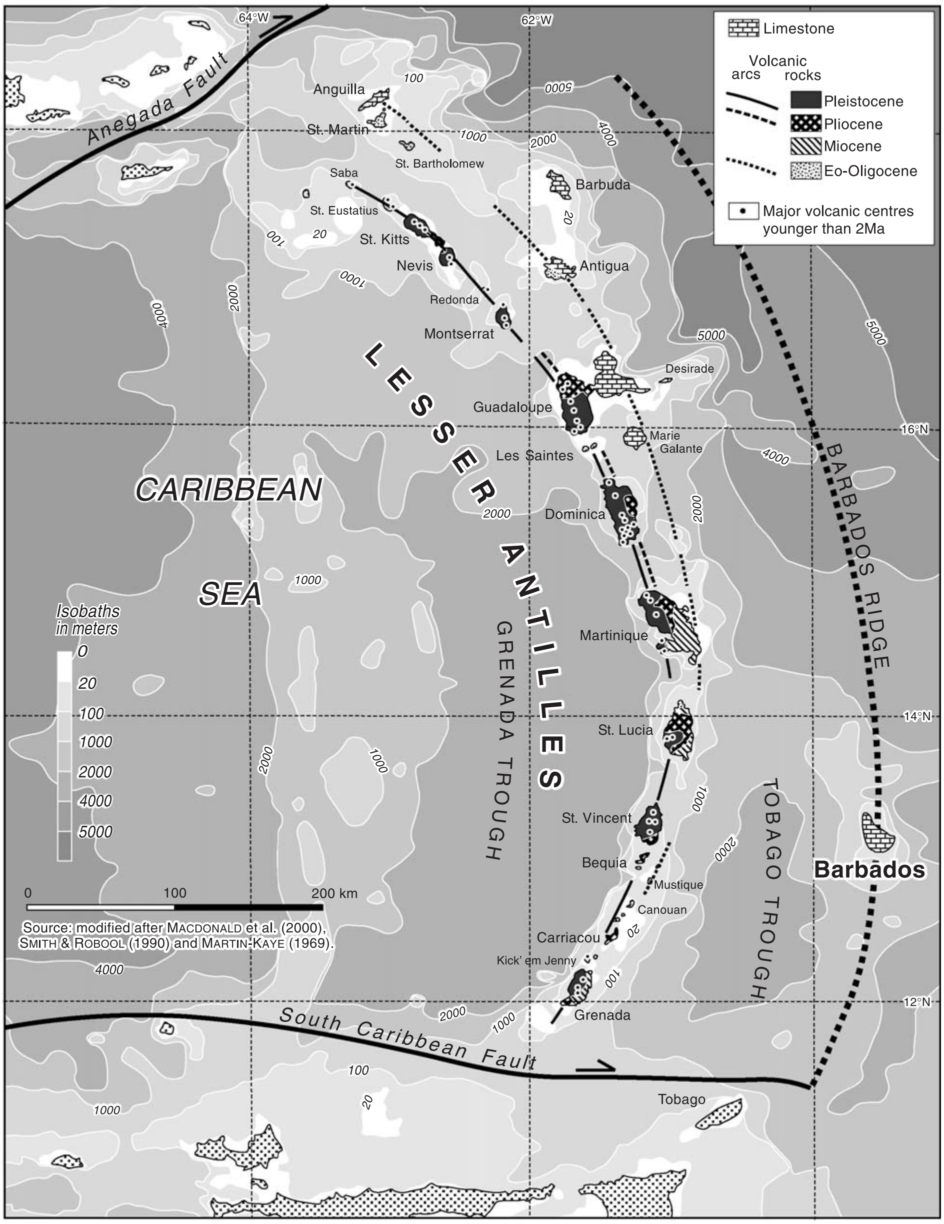

Fig. 1. Geographic location of Barbados. (Modified after: Martin-Kaye, 1969; Smith and Robool, 1990; Macdonald et al., 2000).

ment accumulation has been caused by the subduction of the oceanic crust of the North American Plate beneath the Caribbean Plate since the Late Eocene. The island of Barbados is the only emergent part of the "Barbados Ridge Accretionary Prism", and probably only began to be uplifted from the sea during the Late Early Pleistocene (approx. 1 million years ago; Radtke, 1989). The emplacement of mud diapirs is likely to be responsible for the anomalous elevation of the island above the Barbados Accretionary Prism (Speed, 1990; Speed and Larue, 1982) and for locally differing uplift rates.

Today, Tertiary sedimentary rock is restricted to the Scotland District in the east of Barbados, and covers

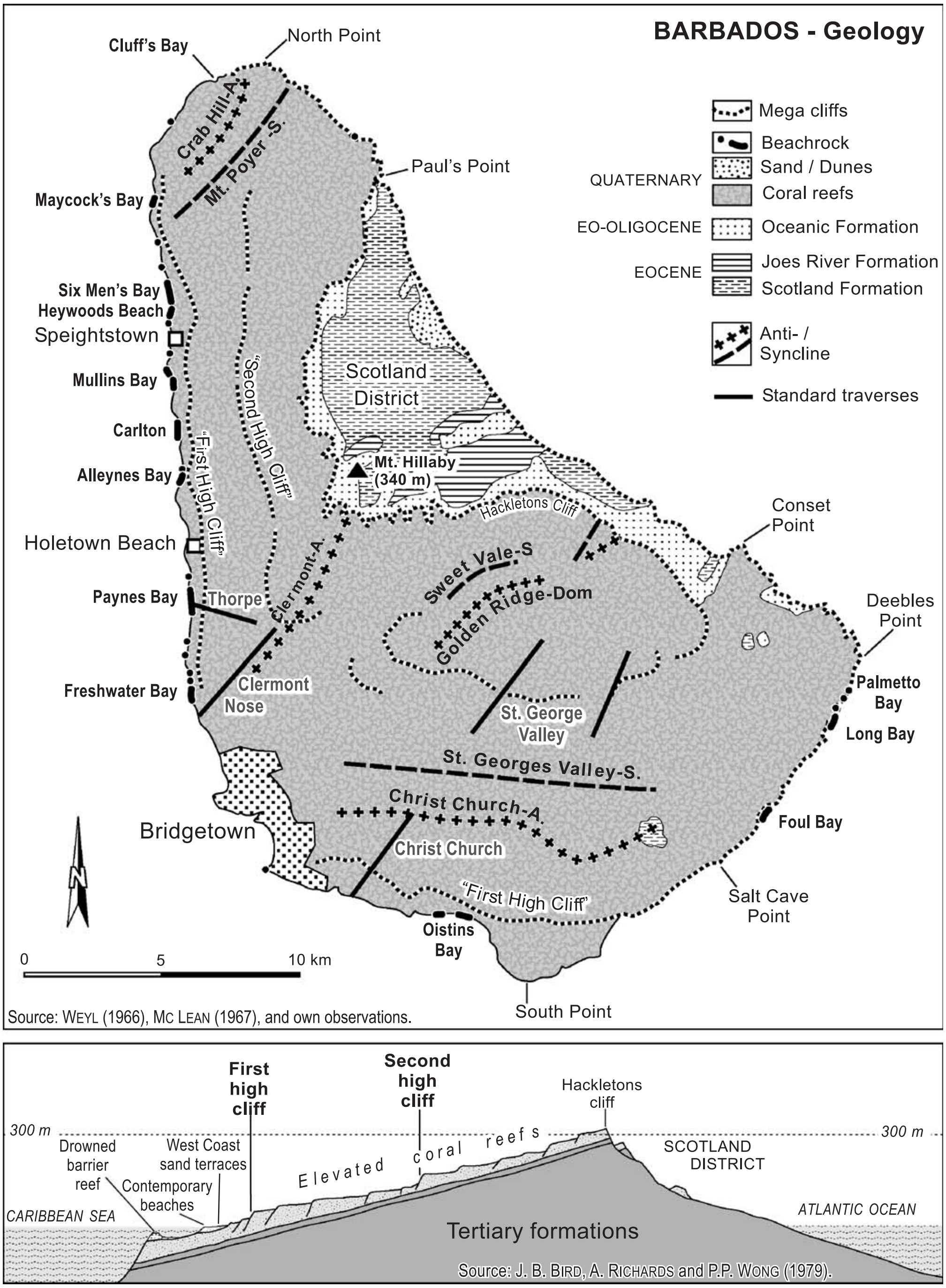

Fig. 2. Geologic map of Barbados. (Sources: Weyl, 1966; Mc Lean, 1967; Bird et al., 1979).

Fig. 3. View of the First High Cliff in southern Barbados. Note Rendezvouz Hill in the background.

approx. 15% of the island (Fig. 2). The remaining 85% of the island is covered by Pleistocene coral limestone which reach thicknesses of up to 130 m and unconformably cover the Tertiary core of the island (Fig. 2). The Pleistocene coral deposits consist of coral reef formations of different ages, which were formed during the long-term uplift of the Barbados Ridge. As emergence has occurred, fringing coral reefs that grew on the sedimentary core of the island have been successively raised above present sea level. Individual reef tracts therefore record glacio-eustatic sea level highstands during the Late and Middle Pleistocene. Some of the older coral reefs on the island are partly anti- or synclinal faulted, whilst others are displaced due to variable uplift rates across the island (Taylor and Mann, 1991).

The coral reef terraces reach their highest elevation (330 m a.s.l.) on the central northern part of the island

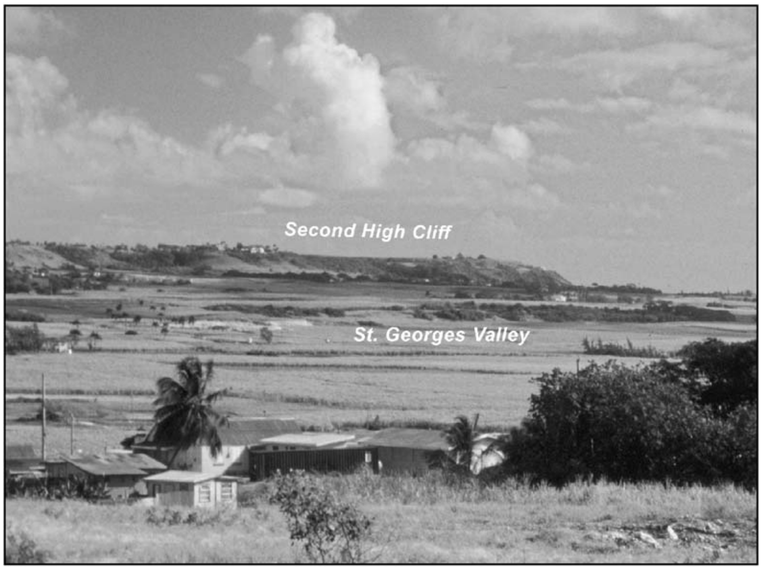

Fig. 4. View of St. George Valley and the Second High Cliff in southeast Barbados.

near Hackletons Cliff (Fig. 2). From here, they descend in several large and small terrace steps in northerly, westerly, and southerly directions towards the Caribbean Sea or the St. George Valley. The coral reef terraces are clearly separated from each other by former cliffs. The two largest reef steps on Barbados are known as the First High Cliff and Second High Cliff (Fig. 2). The First High Cliff is located close to the present coastline and marks the first significant uplift of coral reef terraces above present sea level (between approx. 20 to 61 m a.s.l.) (Fig. 3). The Second High Cliff (Fig. 4) is located at 130 to 200 m a.s.l. (a.s.l. = above mean sea level), and separates the oldest reef structures of the island from the lower reef steps located further west, north, and southeast. Up until the Penultimate Last Interglacial (OIS 7, OIS = marine oxygen isotope stage), the main northern island was separated from the southern island by a channel located in the area of St. George Valley. Thus, the coral reef terraces of the southern part of the island are up to 400,000 years old and significantly younger than the coral reef tracts north of St. George valley and above the Second High Cliff, which are estimated to have been formed as early as 1 Mio. years ago (Radtke, 1989).

2. Previous work

Mesolella et al. (1969) and Broecker et al. (1968) pioneered modern research on uplifted coral reefs on Barbados. Their work was based on stratigraphic data, the distribution of fossil coral reef tracts based on topographic maps and aerial photographs, and on geochronologic studies. Their work focused on the reconstruction of Late and Middle Pleistocene sea level. Numerous subsequent studies concentrated on geochronological investigations along five "standard traverses" which cross different fossil coral reef terraces (Fig. 2). These traverses include the Thorpe and Clermont Nose Traverse on the west coast of Barbados, two traverses in the area between Windsor and Drax Hall in St. George Valley, and the Christ Church Traverse on the south coast. Different dating methods including Uranium/Thorium (U/Th) dating (among others: Gallup et al., 2002; Blanchon and Eisenhauer, 2001), Helium/Uranium (He/U) dating (Bender et al., 1979), and Electron Spin Resonance (ESR) dating (Radtke et al., 1988; Radtke, 1989; Radtke and Grün, 1990) were used for these and subsequent geochronological investigations. Locally, conflicts with the stratigraphic differentiation of the coral reef tracts as originally described by Mesolella (1968) and Bender et al. (1979) were accommodated by minor morphostratigraphic revisions for relatively small areas, as for example those for southern Barbados presented by Radtke (1989) and Ku et al. (1990).

The "Barbados Model", frequently used for the reconstruction of Middle and Late Pleistocene palaeo sea level and global climate change, was essentially derived from studies along the standard traverses described above. In this model stages Barbados I, II, and III are equivalents to the marine oxygen isotope stages 5a, 5c, and 5e from the Last Interglacial (e.g. Edwards et al., 1997; literature review in Radtke, 1989).

3. Methods

This study presents the results of a comprehensive new investigation of the coral reef terraces of Barbados. The project was begun in 1990, stimulated by concerns that the existing morphological and stratigraphic model for the island did not reflect the complex evolutionary history of the Barbados coral reef terraces. In particular, no research had challenged the established morpho- and chronostratigraphic model first proposed by Mesolella (1968) and Bender et al. (1979). Therefore, our work has involved extensive field investigations focusing on the distribution and elevation of coral reef terraces, combined with morphostratigraphical and with geochronological investigations by dating a large number of sample sites.

3.1. Morphostratigraphic methods

This research included the field mapping of former depositional coral reef terraces, former erosional platform terraces (wave-cut platforms), and former cliff lines. Investigations were supported by topographic maps, aerial photographs, lithological surveys, and sampling along road cuts, sea cliffs, and other localities. The following important morphologic criteria determined the delineation and genetic classification of individual reef terraces: (1) Former sea cliffs were identified where they provide clear morphologic borders between reef terrace surfaces of different age. Younger cliffs often have deep notches at their bases. (2) Individual reef crests and their landward reef platform areas were defined using morphological and sedimentary facies data. Some reef platforms are crossed by reef channels or exhibit lower elevated reef lagoons and lagoonal channels, which extend inland. (3) Wave-cut platforms are typically narrow in width and increase in elevation inland. Their surface morphology is unaffected by channels or lagoons (see below).

The elevation of coral reef terraces, including both depositional and wave-cut forms, was measured in the field using a Thommen altimeter with a vertical resolution of 1 m. In addition, morphologic and altimetric field records were checked through manual and digital aerial photo interpretation using true color aerial photographs with a scale of 1:10,000 and a Planicomp P33.

3.2. Electron Spin Resonance (ESR) dating method

The morphostratigraphic investigations on South Barbados were supported by the Electron Spin Resonance (ESR) dating of over 260 coral samples from more than 80 localities (Fig. 14). Due to methodological improvements, the quality of ESR dating results has increased to such an extent that they are comparable to that of Radiocarbon (^{14}C) dating results on Holocene coral from Curaçao (Radtke et al., 2003) and to that of mass spectrometric ^{234}Uranium/^{230}Thorium (TIMS U/Th) dating results for Last Interglacial samples (Schellmann and Radtke, 2001a, 2002; Schellmann et al., 2002). Furthermore, they exceed the accuracy of U/Th dating of older coral samples.

ESR dating was conducted as described by Schellmann and Radtke (2001a). All coral samples were manually ground. Twenty aliquots of 0.2g each with particle diameters between 125 and 250 μm were gamma-irradiated with a ^{60}Co source. The irradiation dose rate ranged from 1 to 2.5 Gy/min. The aliquots of each sample were irradiated in different steps of 9 to 82 Gy up to maximum artificial dose of 178 to 1780 Gy. The irradiation steps and maximum irradiations doses were changed depending on the age of individual coral sample as described by Schellmann and Radtke (2001a). Typical measurement parameters were 25 mW microwave power, 0.5 G modulation amplitude, 22.972 s sweep time, 40 G scan width, 1024 points resolution, and the accumulation of 5 to 10 scans. The ESR signal of $g = 2.0006$ was used for dating. The equivalent dose (D_E) was calculated using the new D-DP procedure described by Schellmann and Radtke (2001a). D_E calculations (Appendix A) were carried out using the program "Fit-sim" by Rainer Grün (version 1993). The annual dose rate (D') of corals depends on the Uranium content as well as on the cosmic dose rate. Double or triple determination of the Uranium content was carried out by Neutron Activation Analysis (INAA: Becquel, Australia, and XRAL, Canada) and for some samples by Inductive Coupled Plasma Mass Spectrometry (ICP-MS: Dept. of Geography/Dep. of Geology, University of Cologne). ESR age calculations were conducted using the software program "Data 7" by Rainer Grün (version V.6, 1999).

This new ESR dating methodology allows for the differentiation between oxygen isotope stages 5a, 5c, and 5e, as well as 7, 9 or 11. Last Interglacial samples can be classified into the main oxygen isotope stages as well as their sub-stages (OIS 5a_1 and OIS 5a_2, OIS 5c and OIS 5e). The accurate differentiation between stages 9, 11 and older remains a challenge due to considerable alterations and recrystallization processes within these older coral samples. Also, the problem of natural "ESR-rejuvenation", which is the recombination of electrons that increases until a natural equilibrium is reached, must be addressed (see e.g. Grün, 1989; Rink, 1997; Jonas, 1997 for principles of ESR dating). Physically, the upper dating limit of the ESR method is defined by this natural equilibrium limit. However, a progressive underestimation of age occurs before this limit is reached. Thus, although only samples with more than 95% Aragonite crystal structure were examined, it was not possible to avoid a significant age under-estimation for coral samples from the Middle Pleistocene. This is despite measuring all ESR samples by X-ray diffraction (Siemens D 5000), and an ESR screen over 300 Gauss, to detect primary or secondary calcite (Schellmann and Kelletat, 2001; Low and Zeira, 1972). Further research is needed to develop a method that recognizes such diagenetic recrystallization and better defines these age rejuvenation effects.

The tendency to under-estimate the ESR age of Middle Pleistocene coral samples was reduced by (1) dating numerous samples from one locality, (2) sampling more than one locality in one coral reef terrace, and (3) using only the oldest ESR dating results for chronostratigraphic interpretation. In the past, the extent of the age rejuvenation effects was assumed to be less than 10,000 years. However, the age under-estimations can be much larger, as illustrated most impressively by the significant change in the range of dating results for the T-8 coral reef terrace on Southern Barbados. For this terrace, preliminary ESR dating results suggested that the terrace was formed during OIS 7 (Schellmann and Radtke, 2001b), however, further ESR dating resulted in a revised age of approx. 300 ka correlating with OIS 9.

This study used the 90th percentile (if the number of ESR dated samples was greater than 20) or the upper quartile (if the number of ESR data was equal or smaller than 20) of all ESR ages from one coral reef terrace for its chronostratigraphic classification (Table 1, Fig. 16). 90th percentile and upper quartile values are ranked values as e.g. the median (50th percentile value). A 90th percentile value means that 10% of a data set are ranked above this value, whereas 25% of a data set are ranked above the upper quartile value. The error ranges of the individual ESR dating results were used for the calculation of the 90th percentile and the upper quartile value. The 90th percentile (upper quartile) value is the mean of the of 90th percentile (upper quartile) value of the maximum ESR data set (ESR age plus error) and the 90th percentile (upper quartile) value of the minimum ESR data set (ESR age minus error). The error range of the resulting mean 90th percentile (upper quartile) value is the deviation from the maximum and minimum 90th percentile (upper quartile) value of an ESR data set. The oldest ESR age was used in cases, where the number of ESR dated samples was too small (less than 4 data) for a calculation of the upper quartile value (Table 1, Fig.

Table 1
Revised morphostratigraphic nomenclature, elevations, and ages for southern Barbados Pleistocene coral reef terraces

Coral reef terraces, T = terrace	$^{18}O/^{16}O$-stage	Elevation of reef crest (m)	Average ages (ky) (*n* = number of datings)		Reef terraces after Bender et al. (1979)	
			ESR age (maximum age)[a]	TIMS $^{230}Th/^{234}U$ ages[b]	$^{230}Th/^{234}U$ age (ky) after* (*n* = number of datings)[c]	
H (Holocene)	1	−1	3.5 (5)	1.7 ± 0.2 (1)	Holocene	
T-1a$_1$	5a-1	2	74 ± 5 (31)	73 ± 0.3 (1)	Worthing (1–4 m)	
T-1a$_2$	5a-2	3	85 ± 7 (10)			
T-1b	5c-1	4–5	104 ± 13 (2)[#]	102 ± 2 (1)		
T-2	5c-2	8–10	104 ± 9 (8)		Ventnor (5–11 m)	MS**** 101 ± 1 (1)
T-3	5c-3	15–17	105 ± 7 (42)			
T-4	5e-1	21–23	118 ± 9 (8)		Maxwell***	AS*** 114–129 (7)
T-5a	5e-2	35–40	128 ± 11 (14)		Rendezvous Hill (35–39 m)	AS*** 121–124 (3)
T-5b	5e-3	40–43	132 ± 13 (15)	128 ± 1 (1)		MS** 122–126 (3) MS***** 129 (1)
T-6a	7-1	46–52	222 ± 21 (23)		Kendal Hill (47–52 m)	MS***** 215 (1)
T-6b	7-2	52–57	>200 (6)			AS* 154–310 (4)
T-7	7-3	60–63	224 ± 22 (11)		Aberdare (65–70 m)	AS* 215–230 (2)
T-8	9-1	72–74	289 ± 22 (23)		Kingsland (77–82 m)	AS* 180–280 (5)
T-9	9-2	81–83	300 ± 40 (15)			
T-10	9-3	90–92	334 ± 34 (6)		Adams Castle (90–94 m)	AS* 180–>320 (4)
T-11	11 (?)	99–101	>310 (4)		Kent, St. Davids (108–113 m)	AS* >350 (1)
T-12	11	108–112	398 ± 46 (27)			
T-13	11	120–122	410 ± 34 (2)[#]		Unnamed (120–122 m)	

Sources: *Bender et al. (1979), **Edwards et al. (1987), ***Ku et al. (1990), ****Bard et al. (1990), *****Blanchon and Eisenhauer (2001).

[a] Maximum ESR age: 90th percentile value, if number of ESR data >20, Upper Quartile value, if number of ESR data ≤ 20 data; [#] = oldest ESR age.

[b] TIMS $^{230}Th/^{234}U$ ages done by Malcom McCulloch (Australian National University): only data with initial $\delta^{234}U$ values >148.5 ± 8‰.

[c] MS = mass-spectrometry $^{230}Th/^{234}U$ ages, AS = α-spectrometry $^{230}Th/^{234}U$ ages.

16). Nevertheless, the timing of coral reef formation would differ only slightly between the calculated 90th percentile and upper quartile values, as illustrated by Fig. 16. These differences lie within the ESR error ranges. All ESR dating results presented in this paper are listed in Appendix A.

Despite the problem of Middle Pleistocene ESR age rejuvenations, these new ESR dating results provide a detailed picture of Late and Middle Pleistocene reef formation for Barbados (see below) which challenges existing chronostratigraphies based on the U/Th dating method alone. Nevertheless, important and still unsolved problems of mass spectrometric U/Th dating of Pleistocene coral include isotope movement and varying $^{234}U/^{238}U$ conditions in the ocean water (Bard et al., 1992).

4. Fossil coral facies, coral reef terraces, wave-cut platforms and notches as sea level indicators

In general, the fossil coral reef terraces on Barbados consist of the morphostratigraphic units and sediment facies illustrated in Fig. 5. The morphological characteristics are similar to those of present fringing reefs in the Caribbean. Notches and beach sand deposits, and reef crests and reef platforms that extend up to the low tide water level provide the most

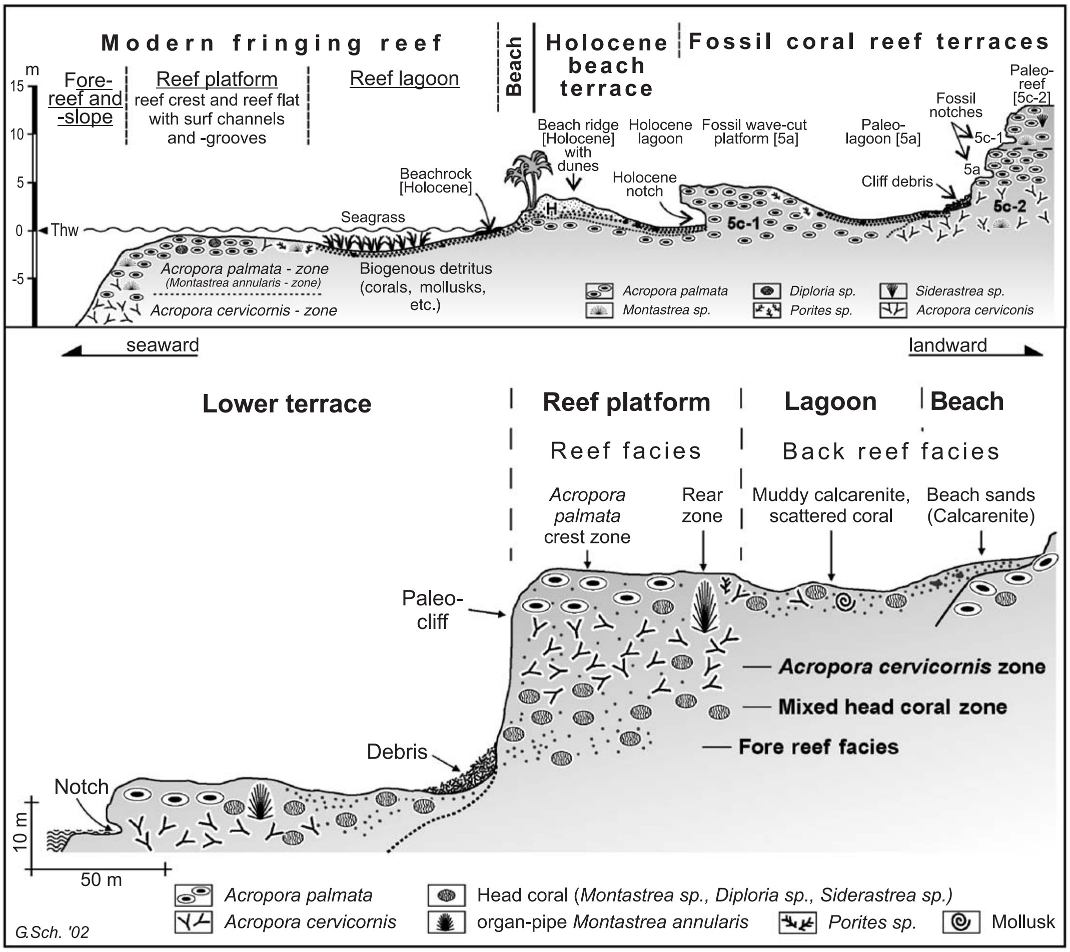

Fig. 5. Sketch of the morphology and coral reef zones of fossil coral reef terraces on Southern Barbados.

important indicators for the reconstruction of Pleistocene sea level change (Schellmann and Radtke, 2002).

4.1. Coral facies patterns

The internal coral facies and zonation of raised Pleistocene reef tracts on Barbados are described by Mesolella et al. (1970), James et al. (1977), Humphrey (1997), Blanchon and Eisenhauer (2001), and others. The facies relationships in the raised reef tracts represent a generalized model, which may vary both vertically and laterally (Humphrey, 1997). Adjacent to the former fore reef calcarenite zone, which is dominated by coral rubble, the reef facies sensu strictu can be subdivided into four major units (Fig. 5) which include (1) the mixed head coral zone containing massive colonies of *Montastrea annularis*, brain coral of different *Diploria* species and, subordinately, species of *Siderastrea* sp. and *Montastrea cavernosa*; (2) the *Acropora cervicornis* zone (Fig. 6) located upwards and landwards of the former fore reef slope, and most commonly containing broken branches of the staghorn coral *A. cervicornis*; (3) the *Acropora palmata* zone (Fig. 6) occupying the former reef crest position (see below); and (4) the near back reef rear zone, where the *A. palmata* crest facies gradually change to a mixed assemblage of corals (e.g. organ-pipe growth forms of *M. annularis*, *Porites* sp., *Siderastrea* sp., *A. cervicornis*) and wave deposited sediments (coral boulders and rubble). A shallow lagoon is located landwards of the rear zone, behind the reef platform, and in the back reef. This lagoon is filled with sandy sediment, some molluscs and, occasionally, solitary corals in living position. Along the former shoreline, the palaeo-lagoon is separated from an older and higher elevated reef terrace by a sea cliff, where a beach and/or a cliff-derived debris zone is sometimes preserved in front of the cliff.

The massive elkhorn coral, *A. palmata*, is the dominant reef builder of former reef crests on Barbados. It is the most common shallow water coral species in the Caribbean and the only coral species which is an appropriate marker for palaeo sea level reconstruction. At present, this species requires strong wave movement and lives in dense colonies in shallow water ranging in depth from maximum of -5 m to low tide level. Fossil and compact *A. palmata* dominated reef crests reaching vertical extensions of 4 to 5 m are present at many localities on southern Barbados. Sometimes, the *A. palmata* crest zone reaches vertical extensions of more than 10 or 20 m as a result of a slow sea level rise during growth. An *A. palmata* reef which is more than 20 m high, and which formed during the Penultimate Interglacial, is exposed in Foul Bay on the southeast coast of Barbados (Schellmann et al., 2002). As noted above, such thicknesses of the shallow water coral zone indicate reef formation against a slow sea level rise. In situ *A. palmata* coral commonly support themselves. Their framework represents a mixture of clasts and in situ colonies (Fig. 6) and the matrix is strongly reduced. Calcareous algal crusts occur within the upper areas of former reef crests, if they have been subject to strong wave action. Geister (1983) described numerous examples for the distribution of calcareous algae on reef crests in the Caribbean. Blanchon and Eisenhauer (2001) used the distinctive asymmetrical thickness of calcareous algae crusts on branches as one important criterion for identifying in situ *A. palmata* dominated reef crest zones. However, compact calcareous algae crusts are rare both on living and on fossil coral on the south coast of Barbados, which is Barbados' leeward side and experiences little wave action. Most fossil corals do not carry any significant calcareous algae crusts.

If collecting coral samples for the purpose of dating, it is important to verify that the sample was taken from an in situ coral formation. Hurricane and tsunami waves can deposit coral rubble and large coral boulders in the back reef area and up to several meters above sea level on top of elevated older coral reef terraces. The latter may be the reason for the anomalously young ESR dating results of coral samples collected in the area to the east of South Point (Fig. 7: sample site XI-75). Here, samples were taken from the surface of the approx. 104 ka old T-2 terrace. The sample site is located immediately behind the sub-stage 5a cliff line of the T-1a_1 coral reef terrace. At that location, it was impossible to verify the in situ position of the samples. The two ESR dating results of 69 ± 5 and 73 ± 8 ka agree well with the age of the 4 m lower elevated T-1a_1 coral reef terrace immediately seaward of the sampling site. However, they are much younger than the approx. 104 ka old T-2 coral reef formation as recorded elsewhere in south Barbados.

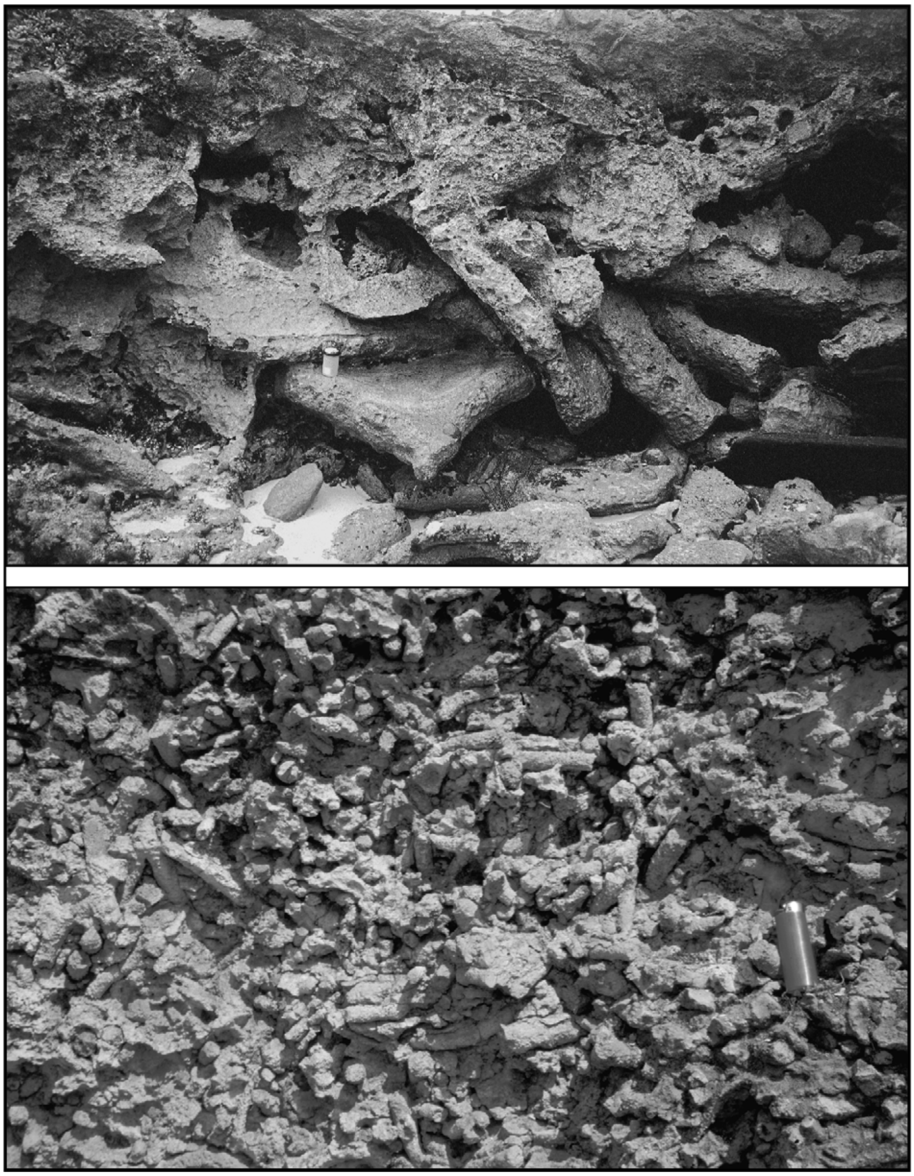

Fig. 6. (Upper photo) Last Interglacial (OIS 5a-1) *A. palmata* reef crest facies with predominately in situ coral supported framework at Inch Marlowe Point, south coast of Barbados; (lower photo) Last Interglacial (OIS 5e) *A. cervicornis* fore reef slope facies at University of the West Indies, west coast of Barbados.

Another example where a reworked assemblage of coral fragments (e.g. head corals lying on their surfaces) have been dated, is sample site Kendal Fort (location XI-80 in Fig. 14). Coral samples here originated from a site at 1 to 3.5 m above the Caribbean Sea where the cliff of the T-2 terrace is undercut by waves. The extremely young ESR dating results with ages between 84 and 96 ka (Appendix A: sample site XI-80) also imply that coral samples had been redeposited by storm waves. The ages are too young when compared to dating results from the well exposed other sample sites

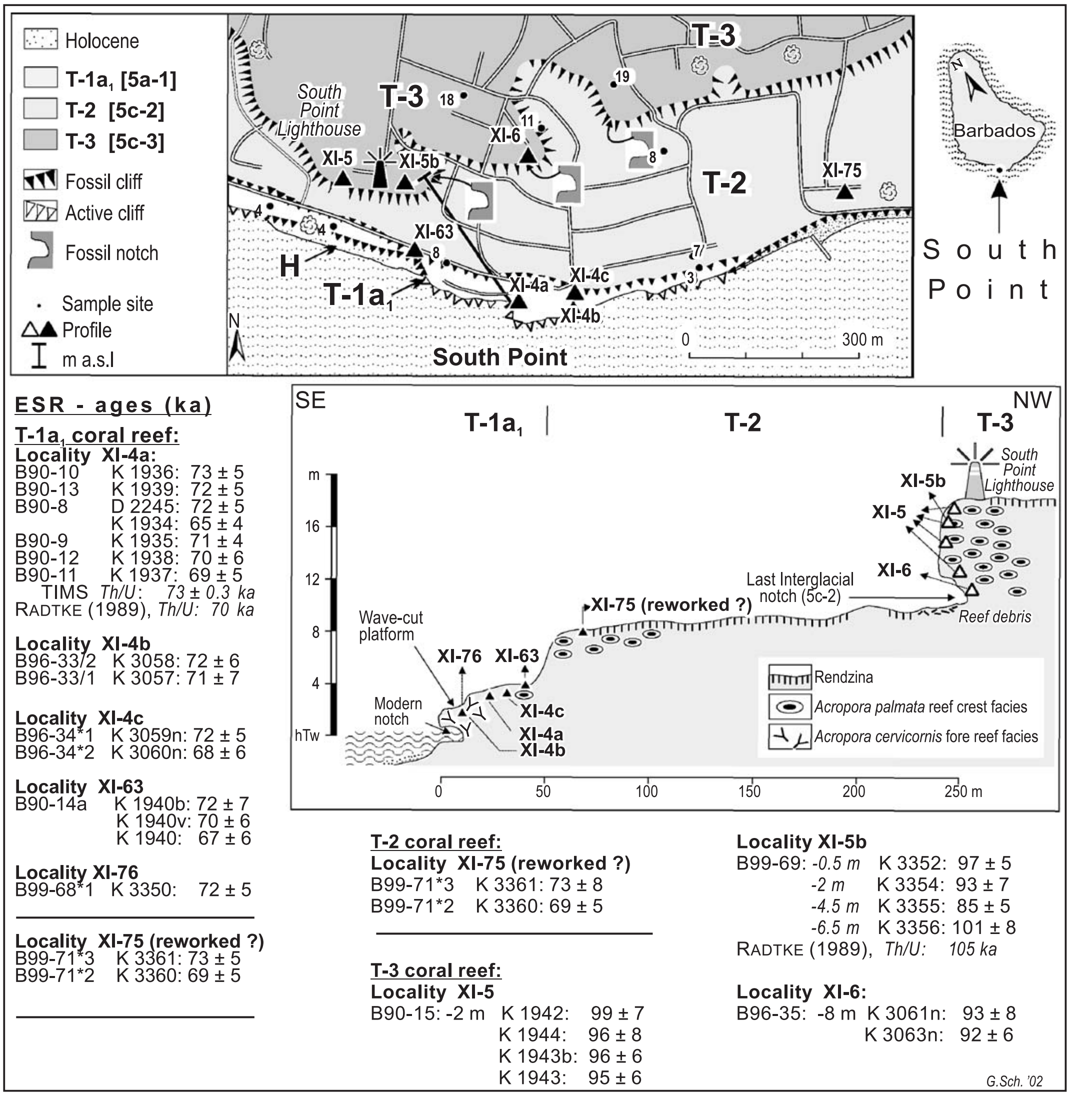

Fig. 7. Coral reef terraces and ESR dating results for South Point area, south coast of Barbados. See Fig. 14 for site location.

(Fig. 14: locations XI-36 to XI-38) on the 104 ka old T-2 coral reef terrace.

4.2. Coral reef terraces and wave-cut platforms

Well-preserved coral reef terraces on Southern Barbados commonly have a steep slope at their seaward part, which comprises a relic cliff or reef slope (Fig. 5). The reef platform, located immediately landward of this slope, typically has little relief and includes a reef crest and back reef plate which may be crossed by reef channels (Fig. 8) that end in a lagoon. The lagoon is often adjacent to a sandy beach, a rocky wave-cut platform, or a steep cliff. This morphological setting provides evidence for a constructional/depositional coral reef terrace, which has grown both seawards and upwards to the former low tide water level.

In contrast to these constructional/depositional landforms some abrasion terraces on Barbados were formed by cliff retreat associated with the erosion of a wave-cut platform into an older coral reef formation. These abrasional forms are younger than the eroded

Fig. 8. View of the T-3 coral reef terrace located at the southern shore of Barbados. Note the intern T-3 reef channel in the front and the built-up T-3 reef crest in the back of the picture.

coral reef formation. Wave-cut terraces are typically narrower than the well-developed depositional coral reef terraces and generally do not exceed 10 to 100 m in width. However, extremely wide wave-cut platforms, formed during some Pleistocene sea level highstands, attain widths of 100 to 400 m, as for example the T-$4_{[7]}$ terrace (Fig. 9) located at the south shore between Paragon and Salt Cave Point. The surfaces of these platforms dip seawards by several meters from their former cliff lines and were clearly formed during slow sea level regression.

The identification and the geochronological classification of wave-cut platforms are difficult. In addition to their commonly narrow width, indicators for the identification of these terraces include (1) the seaward dip in surface elevation of the terrace; (2) the absence

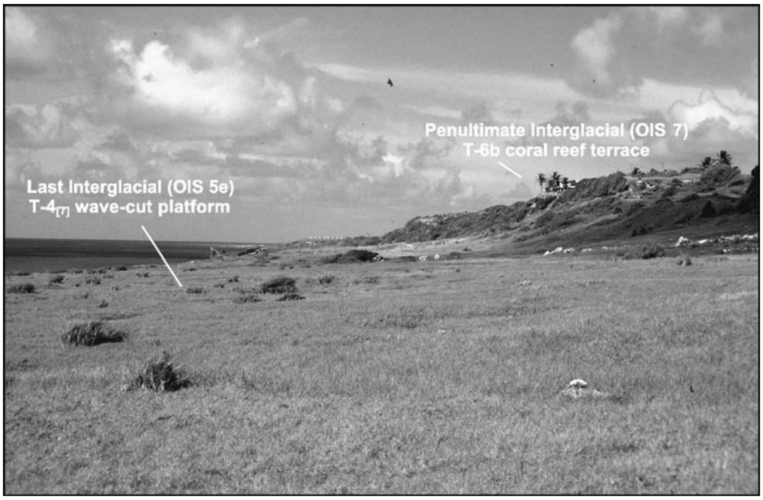

Fig. 9. T-$4_{[7]}$ wave-cut platform located west of Salt Cave Point at the level of the T-4 coral reef terrace. The platform and the palaeo-cliff in the background were formed towards the end of the Last Interglacial transgression maximum (approx. 118 ka). The platform is cut into a Penultimate Interglacial coral reef (T-6b, older 200 ka), which is still preserved and illustrated in the background of the photograph.

of surface channels or lagoons (Fig. 9); and (3) numeric ages which are too old in comparison with the ages of depositional terraces in the surrounding morphostratigraphic context. The later indicator is especially important at localities where small remnants of reef terraces are preserved without any additional morphological features. In such settings, it is impossible to differentiate a depositional coral reef terrace from a wave-cut platform without absolute dating results from surrounding morphological features.

An example of the use of ESR dating to discriminate a wave-cut platform from a depositional terrace is provided by the T-1a$_{[5c]}$ terrace, located at the south coast of Barbados near Oistins (Fig. 10: profile XI-

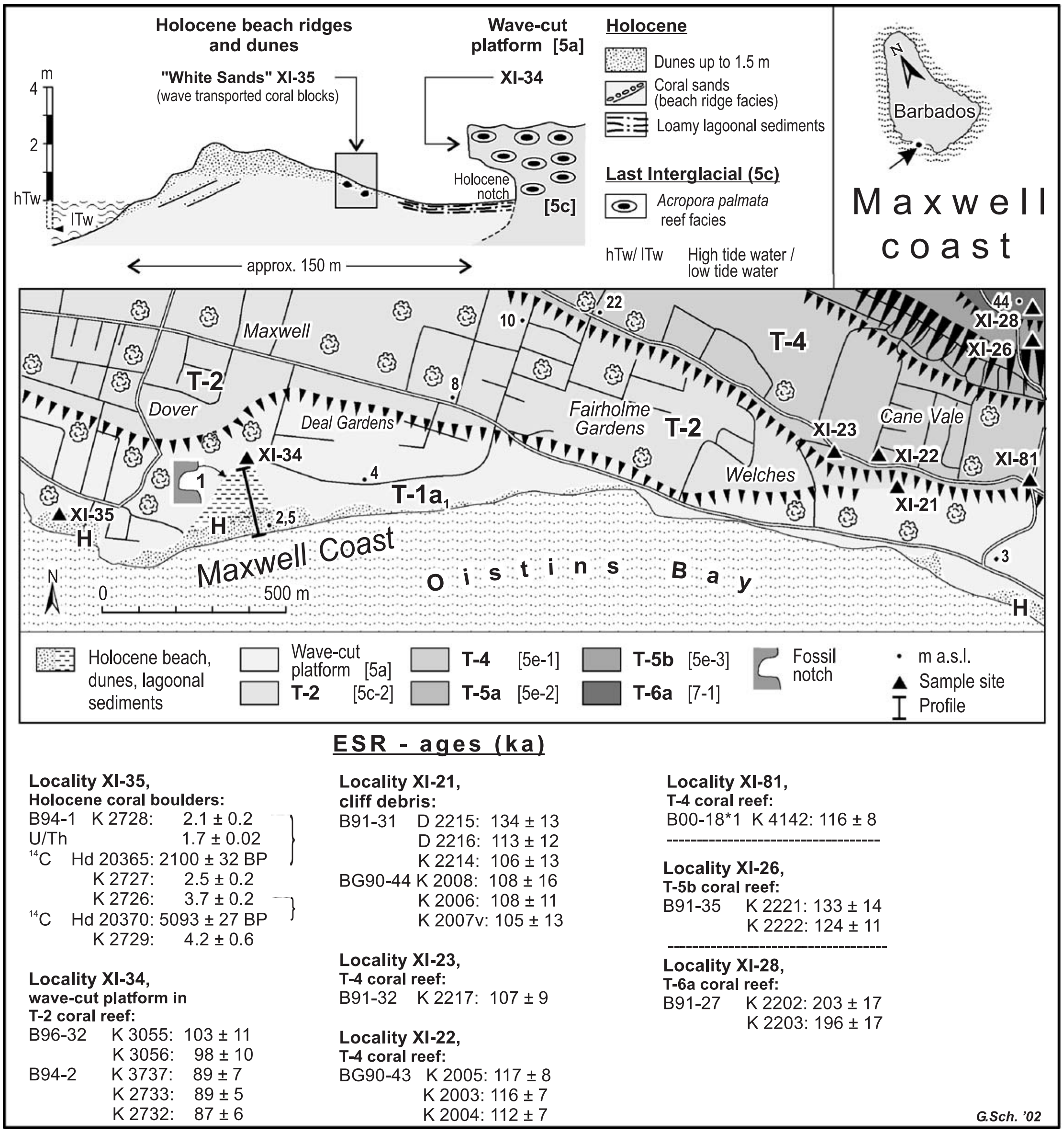

Fig. 10. Coral reef terraces and ESR dating results along Maxwell coast. See Fig. 14 for site location.

34). Here, ESR dates show that the wave-cut platform was abraded into reef crest colonies of OIS 5c old *A. palmata* during OIS 5a. This platform terrace has the same elevation as the reef crest areas of the T-1a terrace dated to OIS 5a and also located along the south coast of Barbados. Both terraces occupy a similar morphological context, yet are composed of coral rocks of quite different ages.

It is important to avoid collecting coral samples for the purpose of dating from in front of former cliffs. In such settings, a small wave-cut rim is usually developed and will typically yield an age determination which exceeds the age of corals exposed at the former cliff. Also, storm layers and cliff debris may be deposited at the foot of such cliffs and result in a mixture of ages. For example, detritus of *A. cervicornis* was sampled at the foot of the T-4 cliff near Oistins (Fig. 10: sample site XI-21). As expected, the ESR dating results split into two groups of ages, comprising (1) ages of approx. 105 to 108 ka, which were concordant with the age of the small T-2 terrace in front of the cliff, and (2) ages between 113 and 134 ka, which were similar to the age of the T-4 coral formation, which is exposed

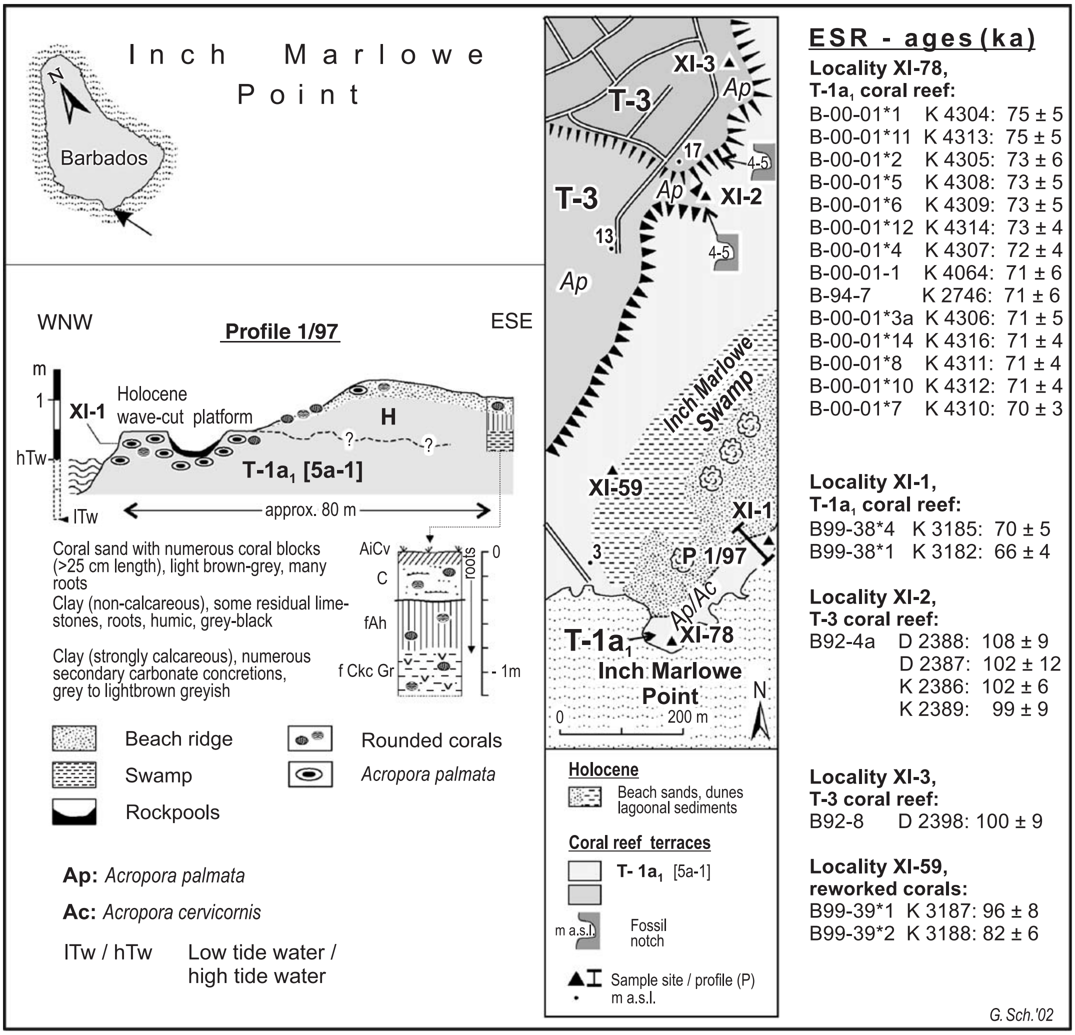

Fig. 11. Coral reef terraces and ESR dating results for coral samples at Inch Marlowe Point. See Fig. 14 for site location.

at the cliff. These dating results disagree with Blanchon and Eisenhower's (2001) geochronological interpretation of similar deposits of well-sorted stick gravel of *A. cervicornis* several hundred meters west of sample site XI-21 at the base of the First High Cliff. These authors mistakingly assumed that these corals were intertidal deposits formed during a brief stage of reef development associated with a rapid sea level fall at the end of the Last Interglacial maximum (OIS 5e).

Another example of a sample site to be avoided when dating corals is provided by age determinations from a small wave-cut rim in front of the T-3 sea cliff located landward of Inch Marlowe Swamp. The swamp is the former lagoon of the T-1a_1 coral reef terrace that was flooded during the Middle or Early Late Holocene (Fig. 11: sample site XI-59). The T-1a_1 coral reef is exposed at the coastline. The sample site is at the same elevation as the T-1a_1 reef platform located at the south coast of Barbados. Two reworked coral boulders embedded in a sandy matrix were dated. As predicted, the two dating results of 82 ± 6 and 96 ± 8 ka were considerably older than the accurately dated age of the preserved T-1a_1 coral reef terrace located to the seaward of the sampling site. The ESR dating results for this terrace scatter between 66 and 75 ka (Fig. 11: sample sites XI-1 and XI-78).

4.3. Notches

Modern and some Late Pleistocene cliffs have more or less developed notches that were generated predominately by bio-erosive processes. Holocene notches located in modern cliffs are incised up to 2 m into the coral limestone at the elevation of present sea level (Fig. 12). Also, Pleistocene notches and sea caves have been preserved along the modern cliff coast, and in higher elevated Late Pleistocene cliffs, mainly at locations that are protected from strong cliff retreat or cliff erosion (Fig. 13; Schellmann and Radtke, 2002).

It is possible to determine the age of a palaeo notch if a fossil coral reef terrace, which formed at the same time as the notch, is present in the foreland. However, the dating of palaeo notches is unreliable if they are located considerably higher than the coral reef terraces preserved in the foreland or if a wave-cut platform is located in front of these notches. Under these circumstances, rough age estimates may be derived from comparing the elevation of the notches to preserved coral reef crests in the greater surrounding area. It is important to consider that tides are small (below 0.7 m) and wave energies reduced at the leeward coast of Barbados. In these regions with little surf, notches mark the elevation of the mean high tide water level and are

Fig. 12. Modern notch north of Crane Beach (southeast coast of Barbados) generated predominately by bio-erosive processes.

Fig. 13. Fossil notches from the Last Interglacial sea level highstand (OIS 5e-1) near Paragon.

located approx. 0.5 to 1 m higher than the highest reef crests of coral reef fringes located in front of the notches.

5. Distribution and chronostratigraphy of fossil coral reef terraces at the south coast of Barbados

Extensive areas of the south coast of Barbados were mapped using the methodology described above. The elevation of preserved coral reef terraces was measured, and more than 260 coral samples (mostly taken from fossil reef crest facies *A. palmata*) were dated using ESR (Figs. 14–16, Appendix A). The oldest coral reefs have been uplifted approx. 120 m above modern sea level. Up to 13 clearly distinguishable coral reef stages are preserved between the present coastline and the center of the southern island near St. Davids. Since a correlation of these new morpho- and chronostratigraphic units to the traditional classification system, including the Worthing Terrace or the Ventnor Terrace, was impossible (Schellmann and Radtke, 2001b), a new nomenclature has been developed. This nomenclature is based on letter–number combinations (Table 1). The lowest and youngest main terrace level, which is located a few meters above present sea level, is called T-1 (T = terrace). The oldest and highest terrace is called T-13.

Prominent reef formations are classified into sub-levels. Sub-levels within a main level are comparable in elevation but may be separated by fossil cliffs. For sub-levels, small letters are added to the terrace identification, such as T-5a and T-5b. Sub-levels were determined along the Christ Church standard traverses (Fig. 13: Profile 1). East of this traverse height differences between sub-levels T-5a and T-5b, and T-6a and T-6b increase to some meters (Fig. 17). Sub-levels T-1a_1 and T-1a_2 are the only features that were classified on geochronologic criteria. Reef crests of both terraces are located at a similar elevation at 2 m or 3 m above modern sea level (Table 1, Figs. 15 and 16). The type locality for these two terraces is located close to the present coast west of Worthing (Figs. 14 and 15). Here, both terraces are morphologically separated by a small palaeo channel or by a wide palaeo lagoon. Based on this morphological context, both terraces may be similar in age and may have formed simultaneously as double fringing reef terraces paralleling the coastline. However, dating results provided different times of formation, including ages of 85 ka for the T-1a_2 terrace, and 74 ka for the T-1a_1 terrace (Table 1, Fig. 16).

Reef terraces preserved by long-term tectonic uplift, such as that recorded on Barbados, typically demonstrate a positive correlation between reef elevation and age. The youngest formations are

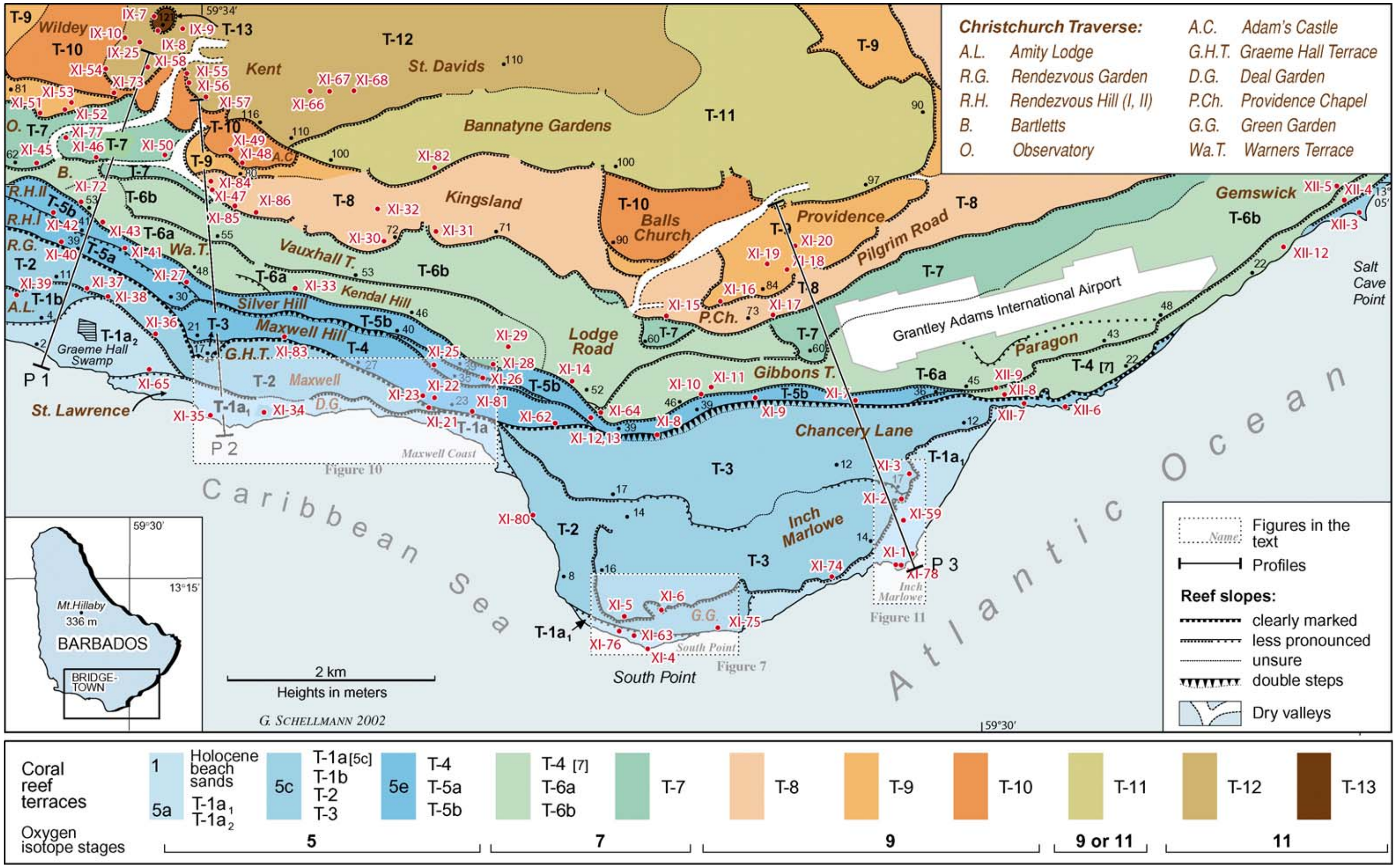

Fig. 14. Overview of the location of Young and Middle Pleistocene coral reef terraces in southern Barbados. The locations of the three traverses and dated sample sites are shown.

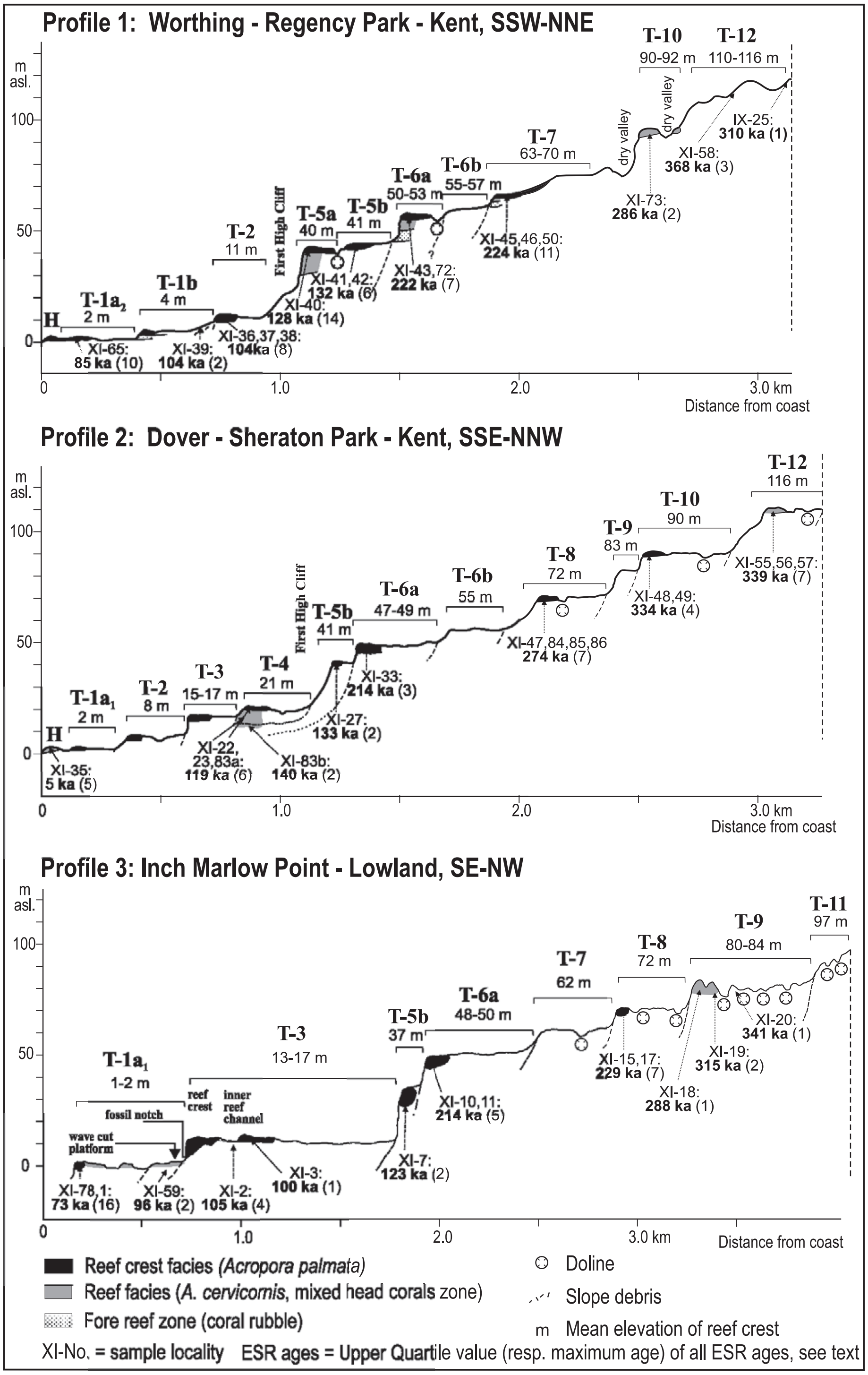

Fig. 15. Morphologic–geologic profile and ESR dating results for coral reef terraces in southern Barbados in the vicinity of the Christ Church Traverse. See Fig. 14 for the location of the three traverses.

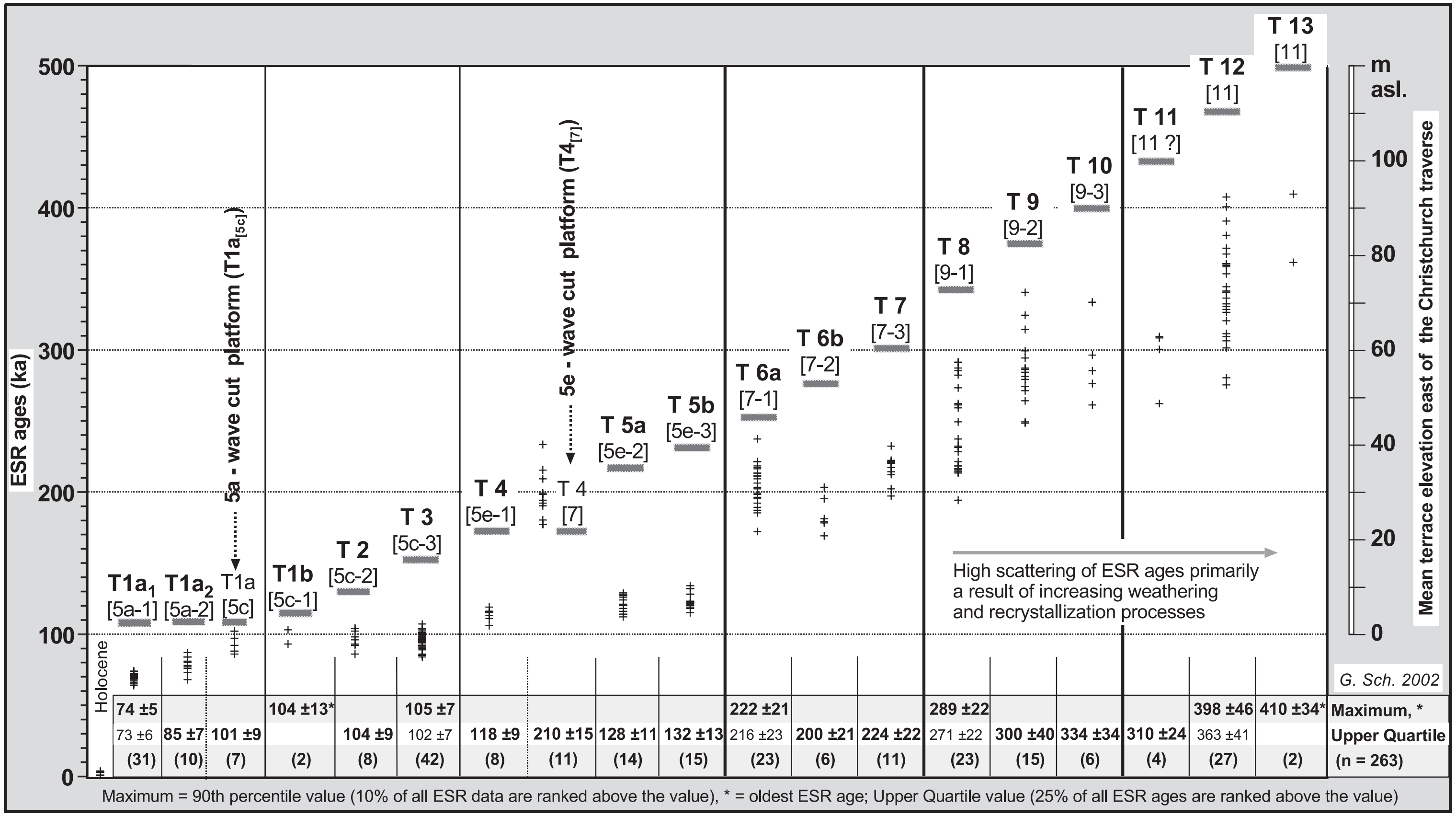

Fig. 16. Elevation and ESR dating results of coral reef terraces in southern Barbados.

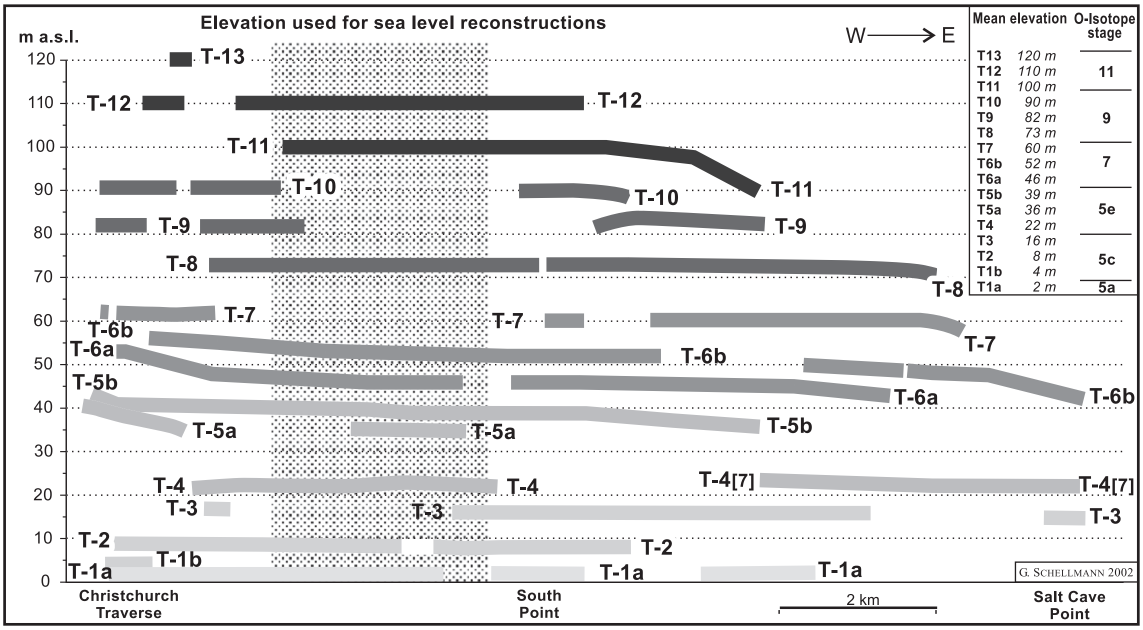

Fig. 17. Elevation of coral reef terraces parallel to the south coast of Barbados.

located at the lowest elevations close to the present coast, with older reef terraces at highest elevations and often at a greater distance inland. Because of the relatively slow rate of uplift in southern Barbados (approx. 0.27 ± 0.02 m/1000a), the youngest reef terrace located above sea level (T-1a$_1$) formed at approx. 74 ka, during the end of the Last Interglacial sea level highstand (OIS 5a-1). The oldest and highest terraces formed during Interglacial sea level maxima date to approx. 410 ka (Table 1), and may be correlated to OIS 11.

Schellmann and Radtke (2001b, 2002) presented a map that compares the newly presented distribution/classification of coral reef terraces in the Christ Church area to the traditional "Barbados Model" as presented by Bender et al. (1979). Table 1 illustrates the differences between the new model presented here and previous models for the south coast of Barbados. ESR ages included in Table 1 represent the upper quartile (dataset ≤ 20) or 90th percentile value (dataset >20) or oldest age of all ESR dating results for coral samples from one terrace level (see above).

The youngest two reef terraces, T-1a$_1$ and T-1a$_2$, are largely comparable to the Worthing reef stage. In the literature, the Worthing stage has been correlated to OIS 5a, and should be 83 ka old (Edwards et al., 1997). However, the terrace had never been dated on the south coast of Barbados. This is the first study to demonstrate that the Worthing stage consists of two distinct depositional terraces; the terrace T-1a$_1$ dated to approx. 74 ka, and sub-level T-1a$_2$ dated to approx. 85 ka (Fig. 14; for details of ESR dating results see Fig. 16). A complete morphological sequence, including reef crest and lagoon, is preserved for T-1a$_1$ at in the St. Lawrence Swamp and Inch Marlowe Swamp areas, and for T-1a$_2$ at the Graeme Hall Swamp area (Fig. 14). At these sites, in situ *A. palmata* reef crest facies commonly have a thickness of more than 1 to 2 m. Furthermore, fossil notches and sea caves, which are elevated approx. 3 to 5 m above modern high tide water level, are preserved at different sites along the cliff coast between South Point and Salt Cave Point (Schellmann et al., 2002). These features may have formed during the development of the T-1a terraces.

The well-known reef stage Ventnor, dated at 101 ka and correlated to OIS 5c in previous studies, encom-

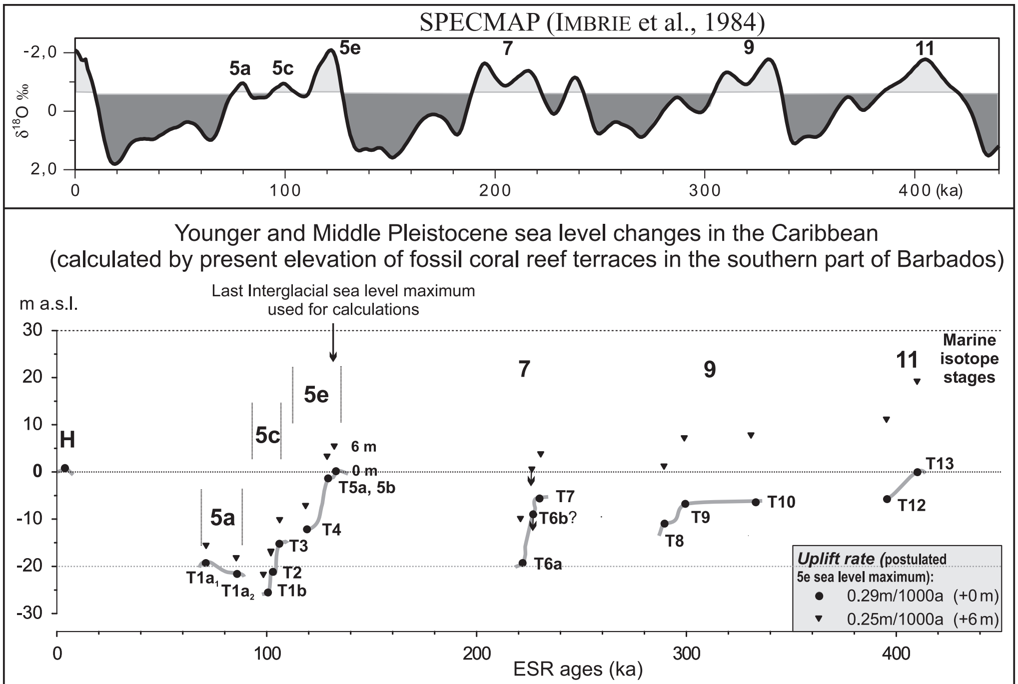

Uplift rate = (elevation of 5e coral reef terrace minus 5e sea level height (0, 6 m)) / (age of the 5e terrace)

Former sea level S_{Tx} = Modern elevation of reef crest Tx minus uplift rate x age of terrace Tx

Period	Terrace	Elevation	Age	$^{18}O/^{16}O$-stage	Sea level (0)	Sea level (+2)	Sea level (+6)
		m	ka		m	m	m
Last Interglacial	T-1a1	2	74	5a-1	-20	-19	-17
	T-1a2	3	85	5a-2	-22	-21	-18
	T-1b	4	104	5c-1	-27	-25	-22
	T-2	9	104	5c-2	-22	-20	-17
	T-3	16	105	5c-3	-15	-13	-10
	T-4	22	118	5e-1	-13	-11	-8
	T-5a	36	128	5e-2	-2	0	4
	T-5b	39	132	5e-3	**0**	**2**	**6**
Penultimate Interglacial	T-6a	46	222	7-1	-20	-16	-10
	T-6b	52	>204	7-2	< -8	< -5	< 1
	T-7	60	224	7-3	-6	-3	4
3rd Interglacial	T-8	73	289	9	-12	-8	1
	T-9	82	300	9	-7	-2	7
	T-10	91	334	9	-8	-3	8
4th Interglacial	T-11	100	-	9 or 11			
	T-12	110	398	11	-8	-2	11
	T-13	120	410	11	-1	5	18

* sea level (m) = Last Interglacial sea level in meter used for estimations
terrace age: Upper quartile or 90th percentile value of ESR data, see text

G.SCH.'03

Fig. 18. Interglacial palaeo sea level changes during the last 400 ka. Calculations are based on the coral reef stages located in southern Barbados.

passes up to three different reef terraces (T-1b to T-3 reef terraces), which were formed before T-1a$_2$ at around 105 ka (OIS 5c). The ESR dating method does not allow for the detection of any age difference between these three terraces. The T-2 and T-3 terraces are widely distributed at the south coast (Fig. 14). In general, their depositional morphology is well preserved and comprises a higher elevated reef crest area associated with lagoons and channels on their landward sides. In contrast, the T-1b terrace is restricted to a small area near Rendezvous Garden (Fig. 14). Houses and gardens cover this area. Its morphologic preservation is poor and the terrace could be a wave-cut platform eroded in the previously formed T-2 reef at the end of OIS 5c.

The T-4 reef terrace has previously been correlated to the Maxwell Terrace by Ku et al. (1990). At Maxwell Hill, T-4 has a well-preserved morphology and displays a sequence of reef crests and lagoonal areas. Further to the east, T-4 has been strongly eroded by younger littoral cliff erosion. Locally, the terrace stretches as a small rim along the slope of First High Cliff (see "reef slope with double steps" displayed in Fig. 14). East of Paragon, T-4 is preserved as an extensive T4$_{[7]}$ wave-cut platform cut into Penultimate Interglacial coral reef limestone (Figs. 9 and 14). Near Paragon, notches and a sea cave are deeply incised at the base of the former T-4 cliffline (Fig. 13). Blanchon and Eisenhauer (2001) hypothesized that this terrace was a submarine fore-reef ridge formed during the Last Interglacial transgression maximum at approx. 129 ka. However, this terrace is the youngest of three constructional coral reef terraces, which were all formed during the maximal Last Interglacial sea level high stand. T-4 formed approx. 118 ka ago when sea level was several meters below present sea level (Table 1, Fig. 18). The two older coral reefs T-5a and T-5b, dated at approx. 128 and 132 ka (Table 1), were formed during the highest Last Interglacial sea level (Fig. 18). The T-5a terrace is best preserved at Rendezvous Hill I, and T-5b between Rendezvous Hill II, Silver Hill and Chancery Lane (Fig. 14).

Coral reefs of different ages are exposed at the First High Cliff (Fig. 14). These include the T-5a reef in the vicinity of the Christ Church Traverse, the T-3 reef to the east, followed by T-4 and finally the T-5b reef near South Point. The First High Cliff was significantly undercut during the formation of the T2- and T3-coral reef terraces, which are approx. 105 ka old (OIS 5c).

The T-6a to T-7 coral reef terraces originated from the Penultimate Interglacial sea level high-stand (OIS 7), approx. 222 to 224 ka ago. Today, these terraces are located in south Barbados at elevations ranging from 46 to 63 m a.s.l. (Table 1, Figs. 16 and 17). The two younger reef terraces T-6a and T-6b are largely comparable to the Kendal Hill Terrace. In comparison, the Aberdare–Kingsland Terrace includes coral reefs from different Interglacials, including reef stage T-7 dated at approx. 224 ka (OIS 7), as well as reef terraces T-8 and T-9 dated approx. 289 and 300 ka (OIS 9), respectively. Based on its elevation, the Adams Castle stage largely correlates to T-10 and is dated to approx. 334 ka (OIS 9). T-11 had not been mapped before.

The stages Kent, St. Davids, and Unnamed, located highest in the southern part of the island (Fig. 14), are classified as T-12 to T-13 in this revised classification scheme (Table 1). Their ages are approx. 398 and 410 ka (OIS 11), respectively (Table 1, Fig. 16).

6. The reconstruction of sea levels during interglacial high stands during the past 400,000 years

Many scientists who base their research on the classical "Barbados Model" assume a 6 ± 4 m higher sea level during the Last Interglacial approx. 130 ka ago (OIS 5e) (e.g. Radtke, 1989). Based on this assumption, sea level alternated between 10 and 20 m below present sea level during subsequent submaxima approx. 80 ka ago (OIS 5a) and approx. 105 ka ago (OIS 5c). These calculations of palaeo sea levels are based on the assumption of a constant rate of uplift for all coastal terraces and an elevation of 6 ± 4 m for the Last Interglacial sea level high stand. Both assumptions require critical evaluation in the light of the new research presented here.

Reef stages from the Last Interglacial transgression maximum (OIS 5e) are located in south

Barbados between 20 and 50 m a.s.l. Assuming that these features record the same highstand, it is an unavoidable conclusion that uplift rates within the study area have varied spatially and, most probably, temporally. One predicament is that the reef terraces within the vicinity of the Christ Church Traverse, which was generally used for sea level calculations in the past, form warped anticlines (Fig. 17). They should, therefore, not be used for sea level calculations. Neither, for similar reasons, should the warped areas of the Clermont Nose Anticline be used. In contrast, the reef terraces preserved to the east of Christ Church standard traverse are not affected by the anticline. These reef crests maintain a constant elevation above present sea level in the area to the west of South Point (Fig. 17). This suggests that a constant uplift has affected this area of the coast. The region located to the east of South Point is also not suited for palaeo sea level estimates, because this region has experienced differentiated tectonic uplift processes. In particular, surfaces of individual older reef terraces descend in eastern direction towards the St. George Valley syncline (Fig. 17).

Fig. 18 summarizes palaeo sea level calculations derived from the region to the east of Christ Church Traverse. These calculations assume different elevations of Last Interglacial sea level highstands, including projections based on sea levels at +6 m, +2 m, and at present sea level. Since the oxygen isotope content in foraminifers from the deep sea was similar for different Interglacials, one may hypothesise that sea levels during the transgression maxima of the previous Middle Pleistocene Interglacials were broadly comparable to Holocene and Last Interglacial sea level highstands. This hypothesis is only supported if one assumes that the Last Interglacial sea level was within the elevation of present sea level or a maximum of 2 m higher (Fig. 18). This would support the postulation of Murray-Wallace and Belperio (1991), who report a 2-m higher sea level during the Last Interglacial sea-level maximum (OIS 5e). The wide-spread assumption that the Last Interglacial sea level was 6 m higher than the present sea level would result in reconstructed sea level heights of between 8 and 18 m for the Third and Fourth past Interglacial (OIS 9 and 11).

The new data presented here suggest that, during the last 400 ka, sea level has oscillated more strongly than previously thought. For example, several substages with sea level elevations between 10 and 25 m below present sea level are preserved on south Barbados from the last two Interglacial sea level highstands (Fig. 18: sub-maxima 5a-1, 5a-2, 5c-1, 5c-2, 5c-3, 7-1). The sea level fall at the end of the relatively short Last and Penultimate Interglacial transgression maximum (Fig. 18: 5e-3 and 7-3; both most likely lasting only few tens of thousands of years) is documented in individual coral reef terraces (Fig. 18: 5e-2, 5e-1, 7-2, 7-3). Ku et al. (1990) suggested that a double highstand during the Last Interglacial was morphologically preserved by the reef stages of the T-5a terrace (the Rendezvouz Hill Terrace) and the T-4 terrace (the Maxwell Terrace). However, the analyses presented here show that both reef stages were formed during the final stages of the transgression maximum after the formation of the T-5b reef (OIS 5e maximum).

Despite the excellent preservation of fossil coral reef terraces on south Barbados, exact statements about the time and duration of palaeo sea level changes older than OIS 5 are limited due to the unsatisfactory resolution of available dating methods. Problems in the recognition of slight diagenetic changes and of Uranium migration in coral samples limit the potential of ESR and Th/U dating. Since Barbados is not influenced by glacio- or hydro-isostatic effects (Peltier, 2002), the palaeo sea levels calculated here should be identical to ice-equivalent eustatic values.

Acknowledgements

We greatly appreciate the excellent help of Anthony Long, who completely polished the English of the manuscript. Thank you to Jack Rink for his comments, which greatly improved the manuscript. We thank the Universities of Cologne and Bamberg, and especially the German Research Foundation for their generous financial support (projects Ra 383/6-1, 6-2, and 6-3) that made this research project, including field work on Barbados and laboratory work at the University of Cologne, Germany, possible.

Appendix A. ESR dating results of Pleistocene coral samples from southern Barbados; see Fig. 14 for site location

Site	Lab. no.	Sample	Elevation, m a.s.l.	Depth		Ali. n	D_{max}, Gy	Uranium		D'		D_E		ESR age	
				cm	±			ppm	±	µGy/a	±	Gy	±	ka	±
IX-07	K-2383	B-92-2a	121	800	200	20	1780	2.45	0.07	918	53	376	21	410	34
IX-08	K-2385	B-92-3	121	500	300	20	1780	3.89	0.26	1408	103	509	71	362	58
IX-09	K-2380	B-92-1a	100	200	100	20	1780	3.33	0.39	1271	124	459	29	361	42
IX-09	K-2381	B-92-1b	100	200	100	20	1780	3.15	0.29	1211	99	436	33	361	41
IX-09	K-2382	B-92-1c	100	200	100	20	1780	2.80	0.14	1115	98	447	34	401	47
IX-09	K-2472	B-92-1b	100	200	100	20	1780	3.15	0.29	1210	101	435	29	359	38
IX-10	K-3011	B-96-4-1	104	300	30	20	1068	3.75	0.35	1362	114	446	32	327	36
IX-10	K-3012	B-96-4-2	104	270	30	20	1068	3.02	0.54	1131	152	374	25	331	50
IX-10	K-3013	B-96-4-3	104	320	30	20	1068	2.46	0.21	967	76	367	48	381	58
IX-10	K-3014	B-96-4-4	104	240	20	20	1068	3.25	0.08	1222	65	417	41	341	38
IX-10	K-3015	B-96-4-5	104	270	30	20	1068	4.35	0.15	1546	87	482	24	312	23
IX-25	K-3207	B-99-47-1	110	100	50	20	534	2.92	0.13	1121	63	348	13	310	21
XI-01	K-3182	B-99-38-1	1	50	30	20	267	3.19	0.14	776	37	51	2	66	4
XI-01	K-3185	B-99-38-4	1	50	30	20	267	3.29	0.20	507	42	56	3	70	5
XI-02	D-2387	B-92-4a-II	13	200	100	20	1780	3.30	0.14	872	63	88	8	102	12
XI-02	D-2388	B-92-4b-I	13	200	100	20	1780	3.30	0.14	890	66	96	3	108	9
XI-02	K-2386	B-92-4a-I	13	200	100	20	1780	3.86	0.08	994	45	102	4	102	6
XI-02	K-2389	B-92-4b-II	13	200	100	20	1780	3.93	0.47	997	86	99	2	99	9
XI-03	D-2398	B-92-8	17	100	50	19	1780	3.30	0.14	891	63	89	5	100	9
XI-04	D-2245	BG-90-8	4	100	50	20	668	3.14	0.16	770	39	55	3	72	5
XI-04	K-1934	BG-90-8	4	100	50	20	445	3.38	0.18	789	40	51	2	65	4
XI-04	K-1935	BG-90-9	4	100	50	20	445	2.85	0.07	713	31	51	2	71	4
XI-04	K-1936	BG-90-10	4	100	50	20	445	3.03	0.25	754	46	55	1	73	5
XI-04	K-1937	BG-90-11	4	100	50	20	445	2.99	0.16	732	37	50	2	69	5
XI-04	K-1938	BG-90-12	4	100	50	20	445	3.13	0.39	761	63	53	2	70	6
XI-04	K-1939	BG-90-13	4	100	50	20	445	3.09	0.30	761	53	55	1	72	5
XI-04	K-3057	B-96-33-1	4	100	50	20	356	3.53	0.35	841	60	60	4	71	7
XI-04	K-3058	B-96-33-2	4	100	50	20	356	3.35	0.21	811	44	58	4	72	6
XI-04	K-3059n	B-96-34-1	4	100	50	20	178	3.15	0.21	772	43	55	2	72	5
XI-04	K-3060n	B-96-34-2	4	50	20	20	178	3.20	0.28	760	53	52	2	68	6
XI-05	K-1942	BG-90-15a	18	200	100	19	356	2.88	0.17	774	43	77	2	99	7
XI-05	K-1943	BG-90-15b	18	200	100	20	445	3.15	0.07	820	36	78	2	95	6
XI-05	K-1943b	BG-90-15b	18	200	100	20	178	3.15	0.07	824	37	79	3	96	6
XI-05	K-1944	BG-90-15c	18	200	100	20	445	3.23	0.16	842	61	81	3	96	8
XI-05	K-3352	B-99-69-1	17	50	30	20	267	3.18	0.10	871	38	84	2	97	5
XI-05	K-3354	B-99-69-3	17	200	50	20	267	3.03	0.28	791	54	74	3	93	7
XI-05	K-3355	B-99-69-4	17	450	50	20	267	3.83	0.13	884	42	75	2	85	5
XI-05	K-3356	B-99-69-5	17	650	50	20	267	3.63	0.35	874	67	89	3	101	8
XI-06	K-3061n	B-96-35-1	18	800	50	19	178	3.57	0.38	820	68	76	3	93	8
XI-06	K-3063n	B-96-35-3	18	800	50	20	178	3.35	0.07	770	37	70	3	92	6
XI-07	D-2191	B-91-22-1	34	200	100	20	668	3.62	0.18	995	76	119	6	120	11
XI-07	K-2193	B-91-22-3	34	200	100	20	668	3.66	0.18	1013	76	124	7	123	12
XI-08	D-2194	B-91-23	39	200	100	20	668	3.43	0.17	986	74	131	9	133	14
XI-10	D-2189	B-91-21-1	46	400	100	20	668	2.65	0.13	866	70	172	18	199	26
XI-10	D-2190	B-91-21-2	46	400	100	20	668	3.23	0.16	1036	84	211	19	204	25
XI-11	D-2185	B-91-19-2	46	300	200	20	668	2.80	0.14	948	76	205	20	217	28
XI-11	D-2186	B-91-19-3	46	300	150	20	668	2.88	0.15	963	76	203	14	210	23
XI-11	K-2184	B-91-19-1	46	300	200	20	668	2.70	0.14	894	70	176	14	197	23
XI-12	K-2069	BG-90-80-1	35	150	50	20	445	3.06	0.32	887	67	110	3	124	10
XI-13	K-2070	BG-90-80-2	39	150	50	20	445	3.35	0.66	934	117	109	3	116	15

Appendix A (*continued*)

Site	Lab. no.	Sample	Elevation, m a.s.l.	Depth		Ali.	D_{max},	Uranium		D'		D_E		ESR age	
				cm	±	*n*	Gy	ppm	±	μGy/a	±	Gy	±	ka	±
XI-14	D-2205	B-91-28-2	50	300	100	20	668	2.84	0.14	932	73	183	14	196	22
XI-14	K-2204	B-91-28-1	50	300	100	20	668	2.84	0.14	943	74	192	9	204	19
XI-15	D-2195	B-91-24-1	70	300	100	20	668	3.03	0.15	1017	82	223	22	219	28
XI-15	K-2066	BG-90-78a	70	200	50	20	445	3.18	0.16	1094	88	251	7	229	20
XI-15	K-2067	BG-90-78b	70	200	50	20	445	3.12	0.16	1082	86	252	9	233	21
XI-15	K-3064	B-96-36-1	70	100	10	20	534	3.80	0.28	1280	86	278	15	217	21
XI-15	K-3066	B-96-36-3	70	100	10	20	534	3.50	0.18	1156	61	225	13	195	16
XI-16	D-2197	B-91-25-1	80	300	100	20	668	3.82	0.19	1351	116	398	50	295	45
XI-16	D-2198	B-91-25-2	80	300	100	20	668	3.13	0.15	1125	94	323	18	287	29
XI-16	D-2199	B-91-25-3	80	300	100	20	668	3.36	0.17	1195	101	341	29	285	34
XI-16	D-2200	B-91-25-4	80	300	100	20	668	3.27	0.16	1181	102	355	40	300	42
XI-17	D-2208	B-91-29-2	70	100	50	20	668	2.83	0.14	998	77	215	19	215	26
XI-17	K-2207	B-91-29-1	70	100	50	20	668	2.84	0.14	1006	77	220	16	219	23
XI-18	D-2229	B-91-39-2	84	300	100	20	668	2.93	0.15	1062	16	305	37	288	42
XI-19	K-3067	B-96-37-1	82	150	20	20	534	3.00	0.57	1110	92	313	23	282	43
XI-19	K-3068	B-96-37-2	82	170	20	20	534	3.04	0.05	1147	57	362	16	315	21
XI-20	K-3069	B-96-37-3	84	150	20	20	534	2.90	0.28	1125	93	383	37	341	43
XI-21	D-2215	B-91-31-2	10	100	50	20	668	3.51	0.16	1031	77	139	8	134	13
XI-21	D-2216	B-91-31-3	10	100	50	20	668	3.47	0.16	966	71	110	8	113	12
XI-21	K-2006	BG-90-44a	10	200	40	20	445	3.79	0.44	998	82	108	7	108	11
XI-21	K-2007v	BG-90-44b	10	200	40	20	445	4.05	0.21	1044	57	109	4	105	13
XI-21	K-2008	BG-90-44c	10	200	40	20	445	3.74	0.80	988	135	107	5	108	16
XI-21	K-2008v	BG-90-44c	10	200	40	20	445	3.74	0.80	1003	138	114	6	113	17
XI-21	K-2214	B-91-31-1	10	100	50	20	668	3.83	0.64	1024	111	108	7	106	13
XI-22	K-2003	BG-90-43a	23	100	20	20	445	3.41	0.16	960	48	111	4	116	7
XI-22	K-2004	BG-90-43b	23	100	20	20	445	3.31	0.13	927	44	104	4	112	7
XI-22	K-2005	BG-90-43c	23	100	20	20	445	2.99	0.16	867	45	102	4	117	8
XI-23	K-2217	B-91-32-1	21	100	50	20	668	3.24	0.16	897	65	96	5	107	9
XI-26	K-2221	B-91-35-1	35	300	100	20	668	2.99	0.15	859	65	114	7	133	14
XI-26	K-2222	B-91-35-2	35	300	100	20	668	3.06	0.15	856	63	106	5	124	11
XI-27	K-3053v	B-96-31-1	37	100	10	20	623	3.20	0.16	840	60	112	5	133	11
XI-27	K-3054i	B-96-31-2	37	200	20	20	312	3.20	0.28	921	64	119	8	129	13
XI-28	K-2202	B-91-27-1	38	300	100	20	668	2.67	0.13	894	70	182	5	203	17
XI-28	K-2203	B-91-27-2	38	300	100	20	668	2.82	0.14	925	73	181	6	196	17
XI-29	K-2201	B-91-26-1	45	300	100	20	668	2.94	0.15	1014	215	241	15	238	53
XI-30	D-2223	B-91-36-1	72	400	200	20	668	3.01	0.15	1076	92	315	37	292	43
XI-30	K-2224	B-91-36-2	72	400	200	20	668	3.10	0.16	1025	84	227	9	222	21
XI-31	K-2226	B-91-38-1	71	400	200	20	668	3.18	0.16	1042	86	226	13	217	22
XI-31	K-2227	B-91-38-2	71	400	200	20	668	3.03	0.15	995	82	213	16	214	25
XI-31	K-4162	B-00-23-1	73	300	30	20	890	3.46	0.20	1200	75	314	9	262	18
XI-31	K-4163	B-00-23-2	73	100	20	20	890	2.72	0.03	1035	49	293	14	283	19
XI-31	K-4164	B-00-23-3	73	400	40	20	890	3.79	0.04	1283	64	334	7	260	14
XI-31	K-4165	B-00-23-4	73	400	40	20	890	3.04	0.09	1085	59	317	11	292	19
XI-32	K-2225	B-91-37	72	400	200	20	668	3.42	0.17	1199	103	342	10	286	26
XI-33	D-2166	B-91-12-1	47	300	100	20	668	3.06	0.15	1017	81	216	11	212	20
XI-33	D-2167	B-91-12-2	47	300	100	20	668	2.70	0.13	898	71	180	8	200	19
XI-33	D-2168	B-91-12-3	47	300	100	20	668	2.74	0.14	927	73	198	11	214	21
XI-34	K-2732	B-94-2-1	2.5	30	20	20	1246	3.27	0.23	876	50	76	3	87	6
XI-34	K-2733	B-94-2-2	2.5	30	20	20	1246	3.38	0.11	906	40	81	3	89	5
XI-34	K-2735	B-94-2-4	2.5	30	20	20	1246	2.92	0.30	820	57	76	3	93	7
XI-34	K-2736	B-94-2-5	2.5	30	20	20	1246	3.88	0.17	1054	52	108	3	103	6
XI-34	K-2737	B-94-2-6	2.5	30	20	20	1246	3.48	0.40	913	71	83	2	89	7

(continued on next page)

Appendix A (*continued*)

Site	Lab. no.	Sample	Elevation, m a.s.l.	Depth		Ali.	D_{max},	Uranium		D'		D_E		ESR age	
				cm	±	n	Gy	ppm	±	μGy/a	±	Gy	±	ka	±
XI-34	K-3055	B-96-32-1	2.5	80	8	20	623	3.15	0.49	821	87	90	4	103	11
XI-34	K-3056	B-96-32-2	2.5	75	0	20	623	2.67	0.33	756	61	74	4	98	10
XI-35	K-2726	B-94-1-1	1	80	40	20	1246	2.86	0.05	465	18	1.7	0.04	3.7	0.2
XI-35	K-2727	B-94-1-2	1	80	40	20	1246	3.82	0.45	550	47	1.34	0.06	2.5	0.2
XI-35	K-2728	B-94-1-3	1	80	40	46	470	3.50	0.28	517	34	1.09	0.02	2.1	0.2
XI-35	K-2729	B-94-1-4	1	80	40	20	1246	3.08	0.67	488	66	2.03	0.08	4.2	0.6
XI-35	K-3083	B-94-1-6	1	100	10	20	623	2.74	0.23	455	28	2.42	0.14	5.3	0.5
XI-36	K-3033	B-96-25-1	9	250	20	20	623	3.66	0.37	916	69	86	5	94	9
XI-36	K-3035	B-96-25-3	9	250	30	20	623	3.42	0.12	842	45	74	3	87	6
XI-36	K-3036	B-96-25-4	9	250	20	20	623	2.89	0.40	778	72	80	3	103	10
XI-37	K-1947	BG-90-18a	10	100	50	20	445	3.05	0.21	833	48	82	3	99	7
XI-37	K-1948	BG-90-18b	10	100	50	20	445	3.31	0.55	882	94	85	4	97	11
XI-37	K-3001	B-96-1-1	10	100	10	20	623	3.75	0.78	963	126	90	2	93	12
XI-37	K-3002	B-96-1-2	10	200	20	20	623	3.15	0.35	850	66	90	4	105	9
XI-38	K-1945	BG-90-16	10	100	50	20	445	3.39	0.16	925	48	98	4	105	7
XI-39	D-2246	BG-90-17	5	100	50	20	668	3.15	0.11	868	40	90	10	104	13
XI-39	K-1946	BG-90-17	5	100	50	20	445	3.29	0.30	872	58	82	4	94	8
XI-40	D-2172	B-91-13-1	39	100	50	20	668	3.31	0.16	949	68	114	11	121	14
XI-40	D-2172A	B-91-13-1	39	100	50	20	668	3.31	0.16	910	70	117	14	122	17
XI-40	D-2173	B-91-13-2	39	100	50	20	668	3.31	0.12	959	45	119	7	125	9
XI-40	D-2242	BG-90-20b	39	400	100	20	668	4.07	0.20	442	58	118	8	113	10
XI-40	D-2247	BG-90-20c	39	800	100	20	668	4.04	0.01	995	46	115	7	115	9
XI-40	K-1952	BG-90-20a	39	400	100	20	445	3.25	0.22	871	53	103	4	119	9
XI-40	K-1953	BG-90-20b	39	400	100	20	445	2.93	0.15	815	63	103	3	127	11
XI-40	K-1954	BG-90-20c	39	800	100	19	356	4.17	0.18	1023	55	117	5	115	8
XI-40	K-2456	B-91-13-2	39	100	50	40	1780	3.35	0.17	982	72	128	5	130	11
XI-40	K-3003	B-96-2-1	39	200	20	20	623	3.40	0.17	968	73	125	5	129	11
XI-40	K-3004	B-96-2-2	39	200	20	20	623	3.54	0.08	980	44	119	8	121	10
XI-40	K-3005	B-96-2-3	39	200	20	20	623	3.25	0.35	927	73	118	5	127	11
XI-40	K-3006	B-96-2-3	39	200	20	20	623	2.92	0.16	851	46	109	5	128	9
XI-40	K-3007	B-96-2-F	39	200	20	20	623	3.73	0.19	1014	90	119	5	117	11
XI-41	K-1955	BG-90-21a	41	30	10	20	445	2.63	0.13	840	58	109	5	129	11
XI-41	K-1956	BG-90-21b	41	30	10	20	445	2.99	0.01	901	37	107	5	119	8
XI-42	K-1949	BG-90-19a	43	100	50	20	445	3.17	0.05	950	41	128	8	135	11
XI-42	K-1950	BG-90-19b	43	100	50	20	445	3.39	0.30	971	66	119	10	122	10
XI-42	K-1951	BG-90-19c	43	100	50	20	445	3.17	0.29	877	38	106	5	121	8
XI-42	K-3090v	BG-90-19c	43	100	10	20	623	3.09	0.01	903	37	111	5	123	7
XI-43	K-2174	B-91-14-1	52	400	200	20	668	2.94	0.15	959	77	198	16	207	24
XI-43	K-2175	B-91-14-2	52	400	200	20	668	3.01	0.26	1055	86	216	9	218	20
XI-43	K-2460	B-91-14-2	52	400	200	20	1780	3.00	0.15	993	81	217	9	219	21
XI-43	K-3092	B-91-14-2	52	400	40	20	1068	2.97	0.04	988	48	220	14	222	18
XI-45	D-2177	B-91-15-2	62	500	200	20	668	3.49	0.17	1126	94	250	19	222	25
XI-45	D-2178	B-91-15-3	62	500	200	20	668	2.82	0.11	930	50	206	19	221	25
XI-46	K-1959	BG-90-23a	64	100	20	20	445	3.46	0.17	1178	93	253	10	215	19
XI-46	K-1960	BG-90-23b	64	100	20	20	445	2.81	0.04	989	44	211	6	213	11
XI-46	K-1961	BG-90-24a	64	100	20	20	445	2.66	0.27	956	74	211	11	221	21
XI-46	K-1962	BG-90-24b	64	100	20	20	445	4.61	0.23	1473	119	292	18	198	20
XI-46	K-3030	B-96-23-2	64	200	20	20	1068	3.57	0.09	1197	60	266	20	222	20
XI-46	K-3031	B-96-23-3	64	180	10	20	1068	3.47	0.18	1190	69	278	16	233	19
XI-46	K-3042	B-96-27-1	64	130	10	20	1068	3.35	0.21	1151	72	256	15	223	19
XI-46	K-3043	B-96-27-2	64	150	10	20	1068	3.57	0.24	1179	70	240	14	203	17
XI-47	K-1964	BG-90-26a	70	150	20	20	445	3.80	0.59	1266	142	274	14	216	27
XI-47	K-1965	BG-90-26b	70	150	20	20	445	4.14	0.84	1393	198	323	14	232	35

Appendix A (*continued*)

Site	Lab. no.	Sample	Elevation, m a.s.l.	Depth		Ali.	D_{max}, Gy	Uranium		D'		D_E		ESR age	
				cm	±	*n*		ppm	±	μGy/a	±	Gy	±	ka	±
XI-48	K-1966	BG-90-27a	89	30	10	20	445	3.62	0.40	1323	114	346	28	262	31
XI-48	K-1967	BG-90-27b	89	30	10	20	445	2.93	0.15	1145	92	340	13	297	27
XI-49	D-2164	B-91-10-1	92	300	100	20	668	3.09	0.04	1152	58	385	19	334	24
XI-49	D-2165	B-91-10-2	92	300	100	20	668	3.11	0.16	1158	101	387	36	334	43
XI-50	K-1963	BG-90-25	72	50	10	20	445	2.62	0.42	956	103	208	7	218	25
XI-52	D-2182	B-91-16-4	83	800	300	20	668	3.61	0.18	1252	115	407	22	325	35
XI-52	K-3044v	B-96-28-1	83	450	40	20	1068	3.15	0.07	1095	57	301	14	275	27
XI-52	K-3045	B-96-28-2	83	450	50	20	1068	3.34	0.23	1125	77	279	15	250	19
XI-52	K-3046v	B-96-28-3	83	450	50	20	1068	3.16	0.06	1104	56	309	16	280	20
XI-53	K-3047v	B-96-29-1	85	100	10	20	1068	3.45	0.35	1252	104	340	17	272	26
XI-53	K-3048v	B-96-29-2	85	100	10	20	1068	3.17	0.23	1158	78	307	10	265	20
XI-53	K-3049	B-96-29-3	85	250	20	20	1068	3.02	0.26	1059	79	263	9	249	21
XI-54	K-3050	B-96-30-1	100	250	20	20	1068	3.47	0.09	1274	69	408	24	321	34
XI-54	K-3051	B-96-30-2	100	250	20	20	1068	3.03	0.10	1141	98	380	27	333	37
XI-55	D-2169	B-91-11-1	105	500	200	20	668	3.83	0.19	1367	123	460	27	337	37
XI-55	K-2170	B-91-11-2	105	500	200	20	668	3.52	0.18	1269	114	433	43	342	46
XI-56	D-2249	BG-90-28a	103	400	100	20	668	3.27	0.51	1191	146	392	30	329	48
XI-56	K-1968	BG-90-28a	103	400	40	20	445	3.42	0.72	1250	111	426	22	341	35
XI-56	K-1969	BG-90-28b	103	400	40	20	445	4.28	0.36	1455	114	401	48	276	40
XI-57	K-1973	BG-90-30a	110	300	30	20	445	3.19	0.16	1158	99	350	19	302	31
XI-57	K-1974	BG-90-30b	110	300	30	20	445	3.10	0.15	1133	98	348	19	307	32
XI-58	D-2252	BG-90-29c	100	600	200	20	668	3.15	0.00	1152	61	424	48	368	46
XI-58	K-1971	BG-90-29b	100	500	50	20	445	2.63	0.13	983	88	348	26	354	41
XI-58	K-1972	BG-90-29c	100	500	50	20	445	3.15	0.16	1160	105	418	14	360	35
XI-59	K-3187	B-99-39-1	2	80	30	20	267	3.36	0.28	896	58	86	4	96	8
XI-59	K-3188	B-99-39-2	2	80	30	25	490	3.47	0.25	874	51	72	3	82	6
XI-62	K-2071	BG-90-81	20	150	50	20	445	3.16	0.57	885	102	101	3	114	14
XI-63	K-1940	BG-90-14a	4	100	50	20	445	3.43	0.38	805	62	54	3	67	6
XI-63	K-1940b	BG-90-14a	4	100	50	20	445	3.43	0.38	805	62	56	3	72	7
XI-63	K-1940v	BG-90-14a	4	100	50	20	178	3.43	0.38	818	63	57	2	70	6
XI-64	D-2187	B-91-20-1	45	200	100	20	668	2.97	0.15	1013	81	217	20	214	27
XI-64	D-2188	B-91-20-2	45	200	100	20	668	2.98	0.15	982	76	187	15	190	21
XI-64	K-2068	BG-90-79	45	200	50	20	445	3.15	0.33	999	79	173	4	173	14
XI-65	K-3037	B-96-26-1	3	20	10	20	623	2.69	0.13	775	35	68	3	88	6
XI-65	K-3038w	B-96-26-2	3	20	10	20	623	2.57	0.17	744	45	63	4	85	8
XI-65	K-3039	B-96-26-3	3	20	10	20	623	3.60	0.18	957	69	82	5	81	7
XI-65	K-3040w	B-96-26-4	3	20	10	20	623	3.39	0.12	908	41	78	3	85	5
XI-65	K-4183	B-00-27-1	3	150	20	20	267	2.63	0.07	673	28	49	2	74	4
XI-65	K-4184	B-00-27-2	3	150	20	20	267	3.60	0.09	868	37	66	2	77	4
XI-65	K-4185	B-00-27-3	3	150	20	20	267	3.10	0.06	775	32	60	2	78	4
XI-65	K-4186	B-00-27-4	3	150	20	20	267	2.90	0.01	749	30	61	4	82	6
XI-65	K-4187	B-00-27-5	3	150	20	20	267	3.15	0.04	789	33	62	2	79	4
XI-67	K-1975	BG-90-31	112	100	30	20	445	2.73	0.14	1084	90	374	23	345	36
XI-68	D-2254	BG-90-32a	102	100	100	20	668	2.64	0.15	1079	68	422	34	391	41
XI-68	D-2255	BG-90-32b	102	100	100	20	668	3.71	0.23	1453	101	593	56	408	49
XI-68	K-1976	BG-90-32a	102	100	50	20	445	2.64	0.15	1008	61	283	21	281	27
XI-68	K-1977	BG-90-32b	102	100	100	20	445	3.83	0.40	1469	134	546	35	372	42
XI-72	K-1957	BG-90-22a	53	100	20	20	445	3.24	0.16	1081	83	209	25	193	27
XI-72	K-1958	BG-90-22b	53	100	20	20	445	3.24	0.16	1073	83	202	10	188	17
XI-72	K-3091	BG-90-22b	53	200	20	20	1068	2.85	0.07	988	48	219	12	222	16
XI-73	K-3009	B-96-3-2	90	200	20	20	1068	3.80	0.01	1355	66	388	28	286	25
XI-73	K-3010	B-96-3-3	90	200	20	20	1068	4.46	0.23	1549	96	429	31	277	26

(*continued on next page*)

Appendix A (*continued*)

Site	Lab. no.	Sample	Elevation, m a.s.l.	Depth		Ali. n	D_{max}, Gy	Uranium		D'		D_E		ESR age	
				cm	±			ppm	±	μGy/a	±	Gy	±	ka	±
XI-74	K-3145	B-99-1	12	200	30	20	267	3.50	0.30	905	61	89	3	98	8
XI-75	K-3360	B-99-71-2	8	50	30	20	267	3.77	0.28	891	53	61	2	69	5
XI-75	K-3361	B-99-71-3	8	50	30	20	267	3.49	0.25	856	49	62	3	73	5
XI-76	K-3350	B-99-68-1	2	20	10	20	267	3.42	0.11	869	38	63	3	72	5
XI-78	K-2746	B-94-7	2	30	10	20	1246	3.37	0.33	841	57	59	3	71	6
XI-78	K-4064	B-00-01-1	1	50	10	20	267	3.41	0.23	1064	48	60	3	71	6
XI-78	K-4304	B-00-01*1	1	15	5	20	267	2.44	0.12	703	31	53	2	75	5
XI-78	K-4305	B-00-01*2	1	15	5	20	267	2.58	0.21	724	41	53	3	73	6
XI-78	K-4306	B-00-01*3a	1	15	5	20	267	2.40	0.15	686	33	49	3	71	5
XI-78	K-4307	B-00-01*4	1	15	5	20	267	2.27	0.11	663	29	47	1	72	4
XI-78	K-4308	B-00-01*5	1	15	5	20	267	2.26	0.13	664	30	48	2	73	5
XI-78	K-4309	B-00-01*6	1	15	5	20	267	2.39	0.23	689	42	50	2	73	5
XI-78	K-4310	B-00-01*7	1	50	10	20	267	2.51	0.03	665	25	47	1	70	3
XI-78	K-4311	B-00-01*8	1	15	5	20	267	2.93	0.03	786	29	56	2	71	4
XI-78	K-4312	B-00-01*10	1	15	5	20	267	2.23	0.07	653	25	46	1	71	4
XI-78	K-4313	B-00-01*11	1	15	5	20	267	3.77	0.19	957	47	72	3	75	5
XI-78	K-4314	B-00-01*12	1	15	5	20	267	3.37	0.17	872	41	63	2	73	4
XI-78	K-4316	B-00-01*14	1	30	5	20	267	3.39	0.17	864	42	60	2	71	4
XI-80	K-4149	B-00-19-3	4	300	30	20	267	2.65	0.13	692	36	65	2	93	5
XI-80	K-4150	B-00-19-4	4	300	30	20	267	2.68	0.13	694	37	64	3	92	6
XI-80	K-4151	B-00-19-5	4	300	30	20	267	2.51	0.13	668	35	64	2	96	6
XI-80	K-4152	B-00-19-6	4	300	30	20	267	3.02	0.16	753	40	66	3	88	6
XI-80	K-4154	B-00-19-8	4	50	20	20	267	2.45	0.14	687	34	58	2	84	5
XI-81	K-4142	B-00-18-1	20	300	100	20	267	3.06	0.15	267	43	97	8	116	8
XI-82	K-4167	B-00-25-1	95	250	50	20	890	3.75	0.02	1301	63	342	18	263	16
XI-82	K-4168	B-00-25-2	95	250	50	20	890	3.60	0.26	1305	94	403	18	309	26
XI-82	K-4169n	B-00-25-3	95	250	50	20	890	3.17	0.15	1160	69	349	14	301	22
XI-82	K-4170	B-00-25-4	95	250	50	20	890	2.65	0.01	1001	48	310	16	310	22
XI-83	K-4136	B-00-17-3	20	700	30	20	267	2.55	0.09	717	36	102	3	142	8
XI-83	K-4137	B-00-17-4	20	700	30	20	267	2.28	0.05	643	30	89	4	138	9
XI-83	K-4140	B-00-17-7	20	600	30	20	267	2.56	0.16	681	41	80	4	117	9
XI-83	K-4141	B-00-17-8	20	250	50	20	267	2.57	0.13	267	38	89	5	120	9
XI-84	K-4156	B-00-20	77	100	20	20	890	3.39	0.17	1216	70	313	5	263	16
XI-85	K-4157	B-00-21	70	250	50	20	890	3.80	0.06	1347	68	388	13	288	18
XI-86	K-4158	B-00-22-1	70	200	20	20	890	3.05	0.08	1105	56	300	14	274	19
XI-86	K-4159	B-00-22-2	70	200	20	20	890	3.34	0.13	1153	62	274	10	238	15
XI-86	K-4161	B-00-22-4	70	200	20	20	890	2.95	0.18	1051	64	262	9	250	17
XII-03	K-1986	BG-90-36a	13	700	100	20	445	3.54	0.08	985	117	188	8	191	24
XII-03	K-1987	BG-90-36b	13	700	100	20	445	3.34	0.27	1048	77	225	10	215	19
XII-03	K-1988	BG-90-36c	13	700	100	20	445	3.12	0.15	980	83	208	7	212	19
XII-03	K-1989	BG-90-36d	13	250	50	20	445	3.54	0.17	925	48	97	3	105	6
XII-03	K-1990	BG-90-36e	13	250	50	20	445	3.45	0.21	904	52	95	3	105	7
XII-03	K-1991	BG-90-36f	13	250	50	20	445	3.63	0.43	940	80	98	3	104	10
XII-03	K-3273A	B-99-57-5	13.5	630	30	50	2670	5.07	0.16	1113	56	95	4	86	6
XII-03	K-3274x	B-99-57-6	13.5	690	30	50	2670	3.84	0.16	926	49	97	2	105	6
XII-03	K-3276	B-99-57-8	13.5	660	30	20	534	4.03	0.06	970	45	100	4	103	6
XII-03	K-3280	B-99-57-12	13.5	1030	30	20	534	3.17	0.24	963	69	200	10	208	18
XII-03	K-3282	B-99-57-14	13.5	470	30	20	534	3.67	0.10	853	42	87	4	97	7
XII-03	K-3283x	B-99-57-15	13.5	390	30	50	2670	3.72	0.25	906	56	86	3	95	7
XII-03	K-3284	B-99-57-16	13.5	300	30	20	534	3.38	0.13	864	43	87	3	101	6
XII-03	K-3285x	B-99-57-17	13.5	60	30	50	2670	3.50	0.71	918	115	84	3	92	12
XII-04	D-2257	BG-90-37a	22	200	100	20	668	3.08	0.09	1024	51	205	19	200	21
XII-04	D-2258	BG-90-37b	22	300	100	20	668	3.03	0.09	980	48	189	20	193	23

Appendix A (*continued*)

Site	Lab. no.	Sample	Elevation, m a.s.l.	Depth		Ali. *n*	D_{max}, Gy	Uranium		D'		D_E		ESR age	
				cm	±			ppm	±	µGy/a	±	Gy	±	ka	±
XII-04	K-1992	BG-90-37a	22	100	50	20	445	3.32	0.25	1114	74	222	9	199	16
XII-04	K-1993	BG-90-37b	22	100	50	20	445	3.38	0.59	1116	133	213	19	191	28
XII-04	K-3262	B-99-56-2	29	50	30	26	534	3.47	0.21	1189	70	249	10	210	15
XII-05	K-1994	BG-90-38a	39	50	20	20	445	3.00	0.15	1011	75	182	2	180	14
XII-05	K-1995	BG-90-38b	39	50	20	20	445	3.33	0.17	1080	81	183	6	170	14
XII-05	K-3252	B-99-55-1	39	100	50	20	267	3.00	0.08	993	46	178	19	179	21
XII-05	K-3254	B-99-55-3	39	100	50	26	534	3.19	0.00	1048	46	190	12	182	14
XII-06	K-2745	B-94-6	13	30	10	20	1246	2.80	0.14	817	55	83	3	101	8
XII-07	K-2390	B-92-5a	13	100	50	20	1780	3.49	0.13	934	44	94	4	101	6
XII-07	K-2391	B-92-5b	13	100	50	20	1780	3.88	0.54	1000	93	96	4	96	10
XII-07	K-3078	B-96-42-2	13	400	40	20	356	3.80	0.28	925	60	89	5	96	8
XII-07	K-3079	B-96-42-3	13	20	10	20	356	3.55	0.35	942	66	81	5	86	8
XII-07	K-3080	B-96-43-1	13	500	50	20	356	3.32	0.12	808	40	77	4	96	7
XII-07	K-3081	B-96-43-2	13	20	10	20	356	3.10	0.42	809	78	92	6	102	9
XII-07	K-3296	B-99-61-3	11.5	870	20	20	267	3.59	0.28	830	57	80	2	97	7
XII-07	K-3297	B-99-61-4	11.5	830	20	20	267	3.00	0.14	730	40	76	3	105	7
XII-07	K-3307x	B-99-61-14	11.5	110	30	50	2670	2.56	0.08	740	33	78	3	105	6
XII-07	K-3310x	B-99-61-17	11.5	170	30	50	2670	3.04	0.14	810	40	79	2	97	5
XII-07	K-3311	B-99-61-18	11.5	390	20	20	267	3.57	0.06	883	39	86	2	98	5
XII-07	K-3312x	B-99-61-19	11.5	90	20	50	2670	3.72	0.45	949	80	86	2	90	8
XII-07	K-3313	B-99-61-20	11.5	90	20	20	267	2.96	0.24	785	50	75	3	93	7
XII-07	K-3314x	B-99-61-21	11.5	50	20	50	2670	3.01	0.38	819	68	75	2	91	8
XII-07	K-3315x	B-99-61-22	11.5	90	20	50	2670	3.38	0.18	870	44	76	3	87	5
XII-07	K-4065A	B-00-02-1	11.5	1100	50	20	267	2.89	0.15	773	36	121	4	153	10
XII-08	K-2392	B-92-6a	29	100	50	20	1780	2.90	0.15	1041	82	243	9	234	21
XII-08	K-2394	B-92-6c	29	100	50	20	1780	2.91	0.16	1022	58	221	10	216	16
XII-08	K-3076	B-96-41	29	100	20	20	356	3.26	0.06	1061	49	189	11	178	13
XII-08	K-3317	B-99-62-2	22	60	20	20	267	3.41	0.02	1112	49	189	13	178	12
XII-09	D-2396	B-92-7a	41	100	50	20	1780	2.80	0.14	864	63	118	7	136	13
XII-09	D-2397	B-92-7b	41	100	50	20	1780	3.30	0.18	908	66	97	4	106	9
XII-09	K-2738	B-94-3-1	41	100	50	20	1246	3.24	0.25	1012	65	157	7	155	12
XII-09	K-2739	B-94-3-2	41	100	50	20	1246	3.03	0.13	845	40	88	3	105	6
XII-09	K-2740	B-94-3-3	41	100	50	20	1246	2.99	0.41	983	94	172	7	175	18
XII-09	K-3321	B-99-63-2	41	400	100	26	534	2.93	0.25	925	67	172	8	186	16
XII-09	K-3322	B-99-63-7	41	400	100	20	267	2.94	0.21	965	65	204	9	212	17
XII-12	K-3288	B-99-59-1	19	50	30	26	534	3.44	0.17	1157	89	226	6	195	16
XII-12	K-3289	B-99-59-2	19	50	30	20	267	3.18	0.17	1060	59	191	9	181	13

References

Bard, E., Hamelin, B., Fairbanks, R.G., 1990. U–Th-ages obtained by mass spectrometry in corals from Barbados: sea level during the past 130,000 years. Nature 346, 456–458.

Bard, E., Fairbanks, R.G., Hamelin, B., 1992. How accurate are the U–Th ages obtained by mass spectrometry on coral terraces. In: Kukla, B.J., Went, E. (Eds.), Start of a Glacial. Springer Verlag, Berlin, pp. 15–22.

Bender, M.L., Taylor, F.W., Matthews, R.K., Goddard, J.G., Broecker, W.S., 1979. Uranium-series dating of the Pleistocene reefs tracts of Barbados, West Indies. Geol. Soc. Am. Bull. I 90, 577–594.

Bird, J.B., Richards, A., Wong, P.P., 1979. Coastal subsystems of Western Barbados, West Indies. Geogr. Ann. 61A (3–4), 221–236.

Blanchon, P., Eisenhauer, A., 2001. Multi-stage reef development on Barbados during the last interglacial. Quat. Sci. Rev. 20, 1093–1112.

Broecker, W.S., Thurber, D.L., Goddard, J., Ku, T.L., Matthews, K.L., Mesolella, K.J., 1968. Milankovitch hypothesis supported by precise dating of coral reefs and deep-sea sediments. Science 159, 297–300.

Edwards, R.L., Chen, J.H., Ku, T.U., Wasserburg, G.J., 1987. Precise timing of the last interglacial period from mass spectrometric determination of thorium-230 in corals. Science 236, 1547–1553.

Edwards, R.L., Cheng, J.H., Murrell, M.T., Goldstein, S.J., 1997.

Protactinium-231 dating of carbonates by thermal ionization mass spectrometry: implications for quaternary climate change. Science 276, 782–786.

Gallup, C.D., Cheng, H., Taylor, F.W., Edwards, R.L., 2002. Direct determination of the timing of sea level change during termination II. Science 295, 310–313.

Geister, J., 1983. Holozäne westindische Korallenriffe: Geomorphologie, Ökologie und Fazies. Facies 9, 173–284.

Grün, R., 1989. Electron Spin Resonance (ESR) dating. Quat. Int. 1, 65–109.

Humphrey, J.D., 1997. Geology and hydrogeology of Barbados. In: Vacher, H.L., Quinn, T. (Eds.), Geology and Hydrogeology of Carbonate Islands. Developments in Sedimentology, vol. 54, pp. 381–406. Amsterdam.

James, N.P., Stearn, C.W., Harrison, R.S., 1977. Field guidebook to modern and pleistocene reef carbonates, Barbados, West Indies. Third Intern. Symp. on Coral Reef, Miami Bead, Florida, pp. 1–31.

Jonas, M., 1997. Concepts and methods of ESR dating. Radiat. Meas. 27, 943–973.

Ku, T.L., Ivanovich, M., Luo, S., 1990. U-series dating of Last Interglacial high sea stands: Barbados revisited. Quat. Res. 33, 129–147.

Low, S., Zeira, S., 1972. ESR spectra of Mn^{2+} in heat-treated aragonite. Am. Mineral. 57, 1115–1124.

Macdonald, R., Hawkesworth, C.J., Heath, E., 2000. The lesser antilles volcanic chain: a study in arc magmatism. Earth Sci. Rev. 49, 1–76.

Martin-Kaye, R.H.A., 1969. A summary of the geology of the lesser Antilles. Overseas Geol. Miner. Resour. 10 (2).

Mc Lean, R.F., 1967. Origin and development of ridge furrow systems in beach rock in Barbados, West Indies. Mar. Geol. 5 (3), 181–193.

Mesolella, K.J., 1968. The uplifted reefs of Barbados: physical stratigraphy, facies relationship and absolute chronology. Diss., Brown Univ., Parts 1 and 2. Philadelphia.

Mesolella, K.J., Matthews, R.K., Broecker, W.S., Thurber, D.L., 1969. The astronomical theory of climatic change: Barbados data. J. Geol. 77, 250–274.

Mesolella, K.J., Sealy, H.A., Matthews, R.K., 1970. Facies geometries within Pleistocene reefs of Barbados, West Indies. Am. Assoc. Pet. Geol. Bull. 54, 1899–1917.

Murray-Wallace, C.V., Belperio, A.P., 1991. The last interglacial shoreline in Australia—a review. Quat. Sci. Rev. 10, 441–461.

Peltier, W.R., 2002. On eustatic sea level history: last glacial maximum to holocene. Quat. Sci. Rev. 21, 377–396.

Radtke, U., 1989. Marine Terrassen und Korallenriffe—Das Problem der quartären Meeresspiegelschwankungen erläutert an Fallstudien aus Chile, Argentinien und Barbados. Düsseld. Geogr. Schr. 27 (Dep. of Geography, University of Düsseldorf).

Radtke, U., Grün, R., 1990. Revised reconstruction of middle and late Pleistocene sea level changes based on new chronologic and morphologic investigations in Barbados, West Indies. J. Coastal Res. 6 (3), 699–708.

Radtke, U., Grün, R., Schwarcz, H.P., 1988. Electron spin resonance dating of the Pleistocene coral reef tracts of Barbados. Quat. Res. 29, 197–215.

Radtke, U., Schellmann, G., Scheffers, A., Kelletat, D., Kasper, H.U., Kromer, B., 2003. ESR and C-14 dating of coral deposited by Holocene tsunami events on Curaçao, Bonaire and Aruba (Netherlands Antilles). Quat. Sci. Rev. 22, 1309–1315.

Rink, W.J., 1997. Electron Spin Resonance (ESR) dating and ESR applications in quaternary science and archaeometry. Radiat. Meas. 27, 975–1025.

Schellmann, G., Kelletat, D., 2001. Chronostratigraphische Untersuchungen litoraler und äolischer Formen und Ablagerungen an der Südküste von Zypern mittels ESR-Altersbestimmungen an Mollusken- und Landschneckenschalen. Essener Geogr. Arb. 32, 75–98 (Dep. of Geography, University of Essen).

Schellmann, G., Radtke, U., 2001a. Progress in ESR dating of young and middle quaternary corals—a new approach of DE determination. Quat. Sci. Rev. 20, 1015–1020.

Schellmann, G., Radtke, U., 2001b. Neue Ergebnisse zur Verbreitung und Altersstellung gehobener Korallenriffterrassen im Süden von Barbados. Bamb. Geogr. Schr. 20, 201–224 (Dep. of Geography, University of Bamberg).

Schellmann, G., Radtke, U., 2002 (with a contribution by Whelan, F.). The coral reef terraces of Barbados—a guide. Barbados 2002—International Conference on ‘‘Quaternary Sea Level Change’’ with field trips and 4th annual meeting of IGCP Project 437 ‘‘ Coastal Environmental Change during sea level highstands: A global synthesis with implications for management of future coastal change’’. INQUA Commission on Coastlines, IGU Commission on Coastal Systems. 26 October–2 November 2002, Barbados (W.I.). Department of Geography, University of Bamberg. 118 pp, with numerous figures and tables.

Schellmann, G., Radtke, U., Potter, E.-K., Esat, T.M., McCulloch, Lambeck, K., 2002. Comparing ESR and TIMS U/Th age measurements of oxygen isotope stage 5c and 5a coral from Barbados. LED 2002, 10th International Conference on Luminescence and Electron Spin Resonance Dating, 24–28 June 2002, Reno (Nevada). Book of Abstracts.

Smith, A.L., Robool, M.J., 1990. A study of an active-island-arc volcano. Geol. Soc. Am., 175.

Speed, R.C., 1990. Volume loss and defluidization history of Barbados. J. Geophys. Res. 95 (B6), 8983–8996.

Speed, R.C., Larue, D.K., 1982. Architecture and implications for accretion. J. Geophys. Res. 87 (B5), 3633–3643.

Taylor, F.W., Mann, P., 1991. Late quaternary folding of coral reef terraces, Barbados. Geology 19, 103–106.

Weyl, R., 1966. Geologie der Antillen. Beiträge zur regionalen Geologie der Erde, Berlin.

G. Schellmann is a Professor in the Department of Geography at the University of Bamberg, Germany. His major research interests include the study of landscape histories (coastal, fluvial and glacial systems) and geochronology (ESR dating technique).

U. Radtke is a Professor in the Department of Geography at the University of Cologne, Germany. His main research interests include geochronology (ESR and Luminescence dating techniques), coastal geomorphology and geoecology.